Identification and Interpretation of Patterns in Rocket Engine Data

FINAL REPORT

Covering the period July 1990 through July 1993

Under NASA Marshall Space Flight Center NAG 8-166
Marshall Space Flight Center, AL 35812

BY:

C.F. Lo, K. Wu and B.A. Whitehead

INSTITUTION:

CSTAR - Center for Space Transportation and Applied Research
UTSI Research Park
Tullahoma, TN 37388-8897
Phone 615-455-9294 or 5884

TABLE OF CONTENTS

Page

SUMMARY 1

1. INTRODUCTION 1

1.1. SSME Cycle 1
1.2. Vibration of Pumps 1
1.3. Methods of Detection 2

2. MONITORING SENSORS AND SPECTRAL DATA 2

3. EXPERT SYSTEM BASED ON THE STATISTICAL METHOD . . . 3

3.1. Pre-processing of Sensor Data 3
3.2. Two Versions of System 3
3.3. System Components 3
3.4. Results of Anomalies Data Analysis 4

4. NEURAL NETWORKS DIAGNOSIS 4

4.1. Neural Network Algorithm Description 5
4.2. Neural Network ANSim Software 5
4.3. Results Obtained from the Experimental Data 5
4.4. Results Obtained from Numerical Simulator 6
4.5. Comments on the Approach of Neural Networks 6

5. CONCLUDING REMARKS 6

REFERENCES 7

ACKNOWLEDGEMENTS 7

FIGURES 8

TABLES 29

SUMMARY

A prototype software system has been constructed to detect anomalous Space Shuttle Main Engine (SSME) behavior in the early stages of fault development significantly earlier than the indication provided by either redline detection mechanism or human expert analysis. The major task of the research project is to analyze ground test data, to identify patterns associated with the anomalous engine behavior, and to develop a pattern identification and detection system on the basis of this analysis.

A prototype expert system which was developed on both PC and Symbolics 3670 lisp machine for detecting anomalies in turbopump vibration data was checked with data from ground tests 902-473, 902-501, 902-519, and 904-097 of the Space Shuttle Main Engine.

The neural networks method was also applied to supplement the statistical method utilized in the prototype system to investigate the feasibility in detecting anomalies in turbopump vibration of SSME.

In most cases the anomalies detected by the expert system agree with those reported by NASA. On the neural networks approach, the results are given the successful detection rate higher than 95% to identify either normal or abnormal running condition based on the experimental data as well as numerical simulation.

1. INTRODUCTION

1.1. SSME Cycle

The Space Shuttle Main Engine (SSME) is a complex and high performance propulsion system. A schematic of the engine with typical 109% power level operational parameters are shown in Figure 1. In the SSME cycle, several turbopumps are involved (Ref. 1). At the propellant inlets, low pressure fuel and oxidizer turbopumps (LPF/OTP) provide the proper pressure head for the two high pressure pumps. Fuel from the high pressure fuel pump discharge flows to cool the main combustion chamber (MCC), nozzle, and other hot components of the engine. The main chamber coolant discharge powers the low pressure fuel turbine (LPFT). The low pressure oxidizer turbine (LPOT) is driven by the oxygen from the high pressure oxidizer pump (HPOP). The oxygen is also fed to a preburner boost pump (PBP) to supply oxidizer at a sufficiently higher pressure level to the preburners. The fuel-rich combustion gases are provided by the two preburners to each respective high pressure turbine. The turbine discharge is mixed with oxygen from the HPOP outlet. Final combustion occurs in the MCC and the combusted gases expand through the supersonic nozzle to produce the thrust.

1.2. Vibration of Pumps

The bearings of the HPFTP and the HPOTP have wear limitations. The HPOTP bearings are more critical since they are bathed and cooled in LOX. During the early days of the SSME program, two major HPOTP failures increased the emphasis of turbomachinery monitoring. One of the key sensors to detect the bearing wear and condition is the strain gauges mounted

internally and externally near the turbopumps. Housing vibration is measured by external accelerometers. In the present study, the major effort is to employ time series data from strain gauges and accelerometers for early detection of turbopump anomalies, such as bearing wear, cage condition, and race condition.

1.3. Methods of Detection

The expert system has been utilized to analyze vibration data from each of the following SSME components: high-pressure oxidizer turbopump, high-pressure fuel turbopump, low-pressure fuel turbopump, and preburner boost pump. The expert system locates and classifies peaks in the power spectral density of each 0.4-sec window of steady-state data. Peaks representing the fundamental and harmonic frequencies in the power spectral density of both shaft rotation and bearing cage rotation are identified by the expert system. The anomalies are detected based on the amplitude of peaks of fundamental and harmonic frequencies. These peaks are found on the basis of the SSME power level, the ratio of cage to shaft rotation, and the required consistency among the different harmonics of each. These data are reduced to the proper format from sensor data measured by strain gauges and accelerometers. By using the statistical method, anomalies are then detected on the basis of sequential criteria and two threshold criteria determined from running averages and standard deviations of nominal data. These sets are individually for the amplitude of each of these peaks: a prior threshold used during the first few windows of data in a test, and a posterior threshold used thereafter.

For the neural network monitoring anomalies, the input layer of a three layers neural network uses the same peaks as that of the statistical method as the basic inputs. The statistical method system will be reported first and the neural network approach later.

2. MONITORING SENSORS AND SPECTRAL DATA

Early monitoring instrumentation consists of external accelerometers and internal strain gauges to monitor the overall loads and vibration levels in the time domain. In many situations, due to the stiffness and damping of the turbopumps, the bearing wear can be directly correlated with the housing vibration as measured by external accelerometers. A strain gauge is mounted to the housing weld of some of the HPOTP units in order to examine the loads at that location. It was found that the bearing characteristics have a close relationship with these weld strain gauge data. The Flight Accelerometer Safety Cutoff System (FASCOS) has been developed and successfully used in ground tests as a redline indicator. In short, the vibration data system is primarily supplied by the turbopump accelerometers and FASCOS.

Power spectral densities were obtained from NASA by FFT (fast Fourier transform) for sequential 0.4-sec windows of data. The typical data for the amplitudes at various frequencies, especially at synchronous frequencies and its harmonics are shown in Figure 2 for high-pressure oxidizer turbopump. A cascade plot of spectral density for an external accelerometer mounted on the high pressure fuel pump is given in Figure 3. It can be seen that there is no appearance of anomaly between 70.0 and 85.0 seconds into the test time frame. The anomalies appear in later time windows around 170.0 seconds.

3. EXPERT SYSTEM BASED ON THE STATISTICAL METHOD

The prototype expert system based on the statistical method has been designed for detecting anomalies in turbopump vibration data from ground tests of the Space Shuttle Main Engine.

3.1. Pre-processing of Sensor Data

Vibration data was provided by NASA in the form of FFT from accelerometers mounted on the oxidizer and fuel pumps. A set of Fortran programs running on the UTSI VAX 11/780 has been developed to read these data tapes in NASA binary format (which is inherently machine-dependent), swaps bytes from the NASA binary format to the VAX internal binary representation, and then converts the data into a portable ASCII format. After initial preprocessing on the VAX, the power spectra are stored in a form which can be quickly sent to any other platform at UTSI. Currently, the data are moved via ethernet to a Symbolics 3670 lisp machine or a PC, and are analyzed as input by the expert systems running on these two platforms.

3.2. Two Versions of System

The earlier operational expert system (Ref. 2) was implemented on a Symbolics 3670 lisp machine. While good preliminary results have been obtained with this implementation, the lisp machine platform and the proprietary lisp language available on this platform both severely limit the portability of the expert system software. Also, the lisp language does not produce run-time code as efficient as that produced by compilers of procedural languages.

In order to maximize the portability of the expert system software and improve the user interface, a re-implementation of its logic in the ANSI standard version of the C programming language was accomplished on PC (Ref. 3). By employing ANSI standard C with the standard C I/O library and making few changes on machine-dependent portion, the expert system can run on any platform which has sufficient memory and disk space for the operation of the software and for the data files it requires.

3.3. System Components

Four major modules of the system (C version) are Frequency Extractor, Anomaly Detector, Hypothesis Generator and User Interface, as illustrated in Figure 4.

The Frequence Extractor is designed to identify the fundamental and harmonic frequencies of both shaft rotation and bearing cage rotation in each FFT window.Firstly peaks representing candidates for the shaft fundamental are reliably found based on an empirical linear fit, for each type of turbopump, of shaft rotation speed to SSME power level as given in Figure 5. The actual shaft and cage fundamental and their harmonics are then identified based on the ratio of cage to shaft rotation and the required consistency among the different harmonics of both shaft and cage. Freq-Extra is also designed to detect the intermittent frequencies whose amplitudes are above a specific value (noise-level).

Anomalies are then detected in Anomaly Detector on the basis of thresholds (prior and posterior)

and sequential criteria set individually for the amplitude of each fundamental and harmonic frequency of both the shaft and the cage. A prior threshold is used during the first few windows of data in a test, while data is first being accumulated for that test. Based on the accumulated data, a posterior threshold is then determined and used for the remainder of the test. Values for the prior threshold of 300% of the amplitude observed in the first window of data, and values for the posterior threshold of 5 standard deviations above the running average of nominal data have been found to give good results for each of the ground tests analyzed to date. For the threshold criteria, anomaly of any identified frequencies is detected when its amplitudes is above its threshold. For sequential criteria, anomaly of any identified frequency is detected when anomalies keep showing in more than three consecutive windows.

The Hypothesis Generator creates hypotheses to apply to either a single sensor or multiple sensors for anomalies data analysis. Hyper-Gene provides recommendations based on the return either from a single sensor detection or multi-sensors identification weighing output of each return. In the case of multi-sensors, the system will determine the severity of anomalies, measured by possibility, good possibility and almost positively, based on the consistence and coherence of each sensor.

The User Interface is graphics-oriented and mouse-driven. It provides users several windows to actively select as screen or hardcopy display, such as Process Status, Single FFT Window, Multiple FFT Windows, Waterfall plots, FFT Recall Windows and Output Files. With a mouse and simple pulldown menus, users can switch among these windows instantly anytime during processing. A sample of interactive (or simulated on-line) session is given in Figure 6. Users first sketch processing plan interactively as in Figure 6a. Figure 6b shows the Process status at the specific time at certain power level. The plot of Single FFT and analysis information is shown in Figure 6c at a specific time. Figures 6d and 6e are the Multiple FFT plots and Waterfall (cascade plots) plots, respectively. FFT recall windows are used for post-test analysis to recall all information in the complete test process, as shown in Figure 6f. The output files save detail records for further examining of anomalies.

3.4. Results of Anomalies Data Analysis

The results of anomalies detected by the system for the data from the ground tests 902-473, 902-501, 902-519 and 904-097 are summarized in Tables 1, 2, 3 and 4, respectively. Results obtained from NASA reports are also listed in a separate column for comparison. The expert system results agree with those stated in the NASA reports, with two exceptions: (1) In test 902-519, HPFTP 50% Sub-synchronized frequency was not detected; and (2) In test 904-097: HPOTP second cage frequency was not detected by the system. These discrepancies require further investigation. The overall results assure us that the current strategy for detecting anomalies works reasonably well for most cases tested.

4. NEURAL NETWORKS DIAGNOSIS

For a specific turbopump component, the fundamental frequency and harmonics for the normal and abnormal conditions have their distinct characteristics as shown in Figures 7 and 8. The neural networks algorithm is a powerful pattern recognition method. Thus, the application of the

neural nets techniques to the HPFTP's data from test 902-501 and 902-519 allows us to examine the feasibility in diagnosing the anomalies (Ref. 4).

4.1. Neural Network Algorithm Description

A three-layer Back-Propagation (BP) Neural Network has been selected for the present study. Multilayer BP networks have been studied extensively and are widely used for pattern classification. Multilayer networks are able to classify non-linearly separable classes. In the present case, a three layer network is utilized including input layer, hidden layer and output layer. A 3-layered (input, hidden,output), fully connected, feed-forward network as shown in Figure 9. The normalized data sets are utilized. Both input and output are continuous-valued (between -0.5 and 0.5) vector. The outputs generated by the network are compared with the desired or target outputs. Errors are computed from the differences, and the weights are changed in response to these error signals as dictated by the Generalized Delta Rule (Ref. 5). Thus, a BP network learns a mapping function by repeatedly presenting patterns from a training set and adjusting the weights. A commercial neural network program named ANSim (Ref. 6) is utilized for the training process as well as the testing process.

The Training Procedure is in the iterative fashion. It loops repeatedly over the set of training patterns until the total root mean square (RMS) error for all patterns is less than the specified value, e.g. 0.1. The Testing Procedure is forward feed processing.

4.2. Neural Network ANSim Software

A commercial neural network program named SAIC ANSim 2.30 is a graphics oriented, menu-based artificial neural system (ANS) simulation program, which provides a complete complement of neural model development, allocation and analysis capabilities, including a powerful ANS creation, training, execution and monitoring tool. ANSim enables users to quickly implement and utilize ANS models using 13 paradigms such as Back Propagation (BP), Hopfiled Network, etc. ANSim enables the user to configure any number of ANS neural networks. It drives each network with a sequence of training and/or input data. For each model, ANSim will (1) monitor the response, (2) capture the output, and (3) save the configuration for later re-use. ANSim is integrated under Microsoft Windows to provide an effective, easy-to-use interface. A Floating Point Processor for ANSim is available to speed up the training clock time. A PC 386 (VGA or EGA monitor) with the SAIC's Delta Floating Point Processor, which is a 22 MFlop AT bus compatible processor, allows for high speed Neural Network Systems training and processing.

4.3. Results Obtained from the Experimental Data

The typical data sets are obtained by the pre-processor module as shown in Figure 10. consisting of synchronous frequency samples of normal and 240-hz abnormal data sets for sensor 696 and 698 of Test 902-501. The sensor 613 of Test 902-519 for Synchronous and Sub-synch frequency data is shown in Figure 11. The initial selected component for the current study is the HPFTP. The vibration data from ground tests 902-501 and 902-519 for the HPFTP as shown in Figures 7 and 8 are utilized to the current vibration anomalies detection. The reserved testing data, which have not been used for training the network in the same test, are applied to assess the

effectiveness and feasibility of the network approach. The successful detection rate is higher than 95% to identify either normal or abnormal running condition. The results have indicated that the application of Neural Network to the available SSME vibration data sets in diagnosing existing faults in the data is a viable method. To reassure the neural network's effectiveness, the investigation of more cases and more fault scenarios are required. Since the limited ground test data is available, the study using the data generated from a NASA/MSFC's numerical simulator is reported in the next section.

4.4. Results Obtained from Numerical Simulator

The current simulated data were provided by Fred Kuo at MSFC from a numerical simulator (Ref. 7) developed at NASA/MSFC. Three data sets are obtained from the Numerical Simulator. These cases received from NASA on Nov. 15, 1992 and Feb. 18, 93 have been studied. Two of these sets are "Rotor.DB" and the other is "Rotor.UB". The displacement response in the Y and Z direction and the side-force in the Y and Z direction vs. dimensionless time as shown in Figures 12, 13 and 14, respectively. These sample numerical data were analyzed by fast Fourier Transform in the spectrum plots with three different sizes of window for sample response-amplitude data plotted in Figures 15, 16 and 17. The side-force sample data are shown in Figures 18, 19 and 20. The sample results are given in Tables 5 and 6 for both Y-response and Y-force of Rotor.UB and Rotor.DB, respectively. Even with the limited data base, the successful rate is very reasonable after 300 training cycles in SAIC ANSim 2.30.

4.5. Comments on the Approach of Neural Networks

For the training process of the Neural Networks, the clock time of computer computation on a PC-386 with Floating Point Processor is less than 1 minute. The testing time of the feed-forward process is near real time in the present case. This is important to know this computation time for planning on-line or off-line operation in addition to its ability to identify the correct anomalies.

The limited application of neural networks to the HPFTP and the simulation data have shown the effectiveness and feasibility to diagnose the anomalies of turbopump vibrations. The further investigation on data from a numerical simulator and actual experiment data is warranted in the future.

5. CONCLUDING REMARKS

Automatic detection of anomalies in Space Shuttle Main Engine Turbopumps has been implemented as a prototype software system on a Symbolics 3670 lisp machine and on a PC. The system has demonstrated its capability in detecting anomalies in turbopump vibration data earlier than the indication provided by the redline detection mechanism. The present strategy based on the statistics distribution of data in detecting anomalies for SSME turbopumps seems to be working well, even though some limited cases require further study. On the other hand, the limited application of neural networks to the HPFTP has also shown the effectiveness and feasibility to diagnose the anomalies of turbopump vibrations. The further investigation on data from experimental data sets and the numerical simulator is recommended before implementing

for the on-line ground testing.

REFERENCES

1. Rockwell International "SSME Orientation (Part A--Engine), Space Transportation System Training Data," Course No. ME 110(A) RIR, January 1991

2. L. Pereira and M. Ali, " Identification and Detection of Anomalies Through SSME Data Analysis," CASP, 2nd Technical Symposium Proceeding, November 1991

3. C. F. Lo, B.A.Whitehead, and K. Wu, "Automatic Detection of Anomalies in Space Shuttle Main Engine Turbopumps", AIAA Paper No. 92-3329, Joint Propulsion Conference, July 1992

4. C. F. Lo, K. Wu, and B.A.Whitehead, "Anomaly Detection of Turbopump Vibration in Space Shuttle Main Engine Using Statistics and Neural Networks", AIAA Paper No. 93-1777, Joint Propulsion Conference, June 1993

5. D. E. Rumelhart, G. E. Hinton, and R. J. Williams "Learning Internal Representations by Error Propagation", Parallel Distribution Processing, Vol. I, 1986

6. Science Application International Corp. "ANSim Artificial Neural Systems Simulation Program", April, 1989

7. S. G. Ryan "Limit Cycle Vibrations in Turbomachinery", NASA Technical Paper 3181, December 1991

ACKNOWLEDGEMENTS

This research was supported by the Structure and Dynamics Laboratory of NASA-MSFC Grant No. NAG 8-166. The investigators would like to thank Pat Vallely, Technical Monitor, NASA/MSFC, Tom Fox and Fred Kuo of NASA/MSFC and Carlyle Smith for their technical advice. To Dr. M. Ali who served as the principal investigator before August 1991 and Ms. L. Pereira who coded the expert system on a Symbolics machine, we express our appreciation.

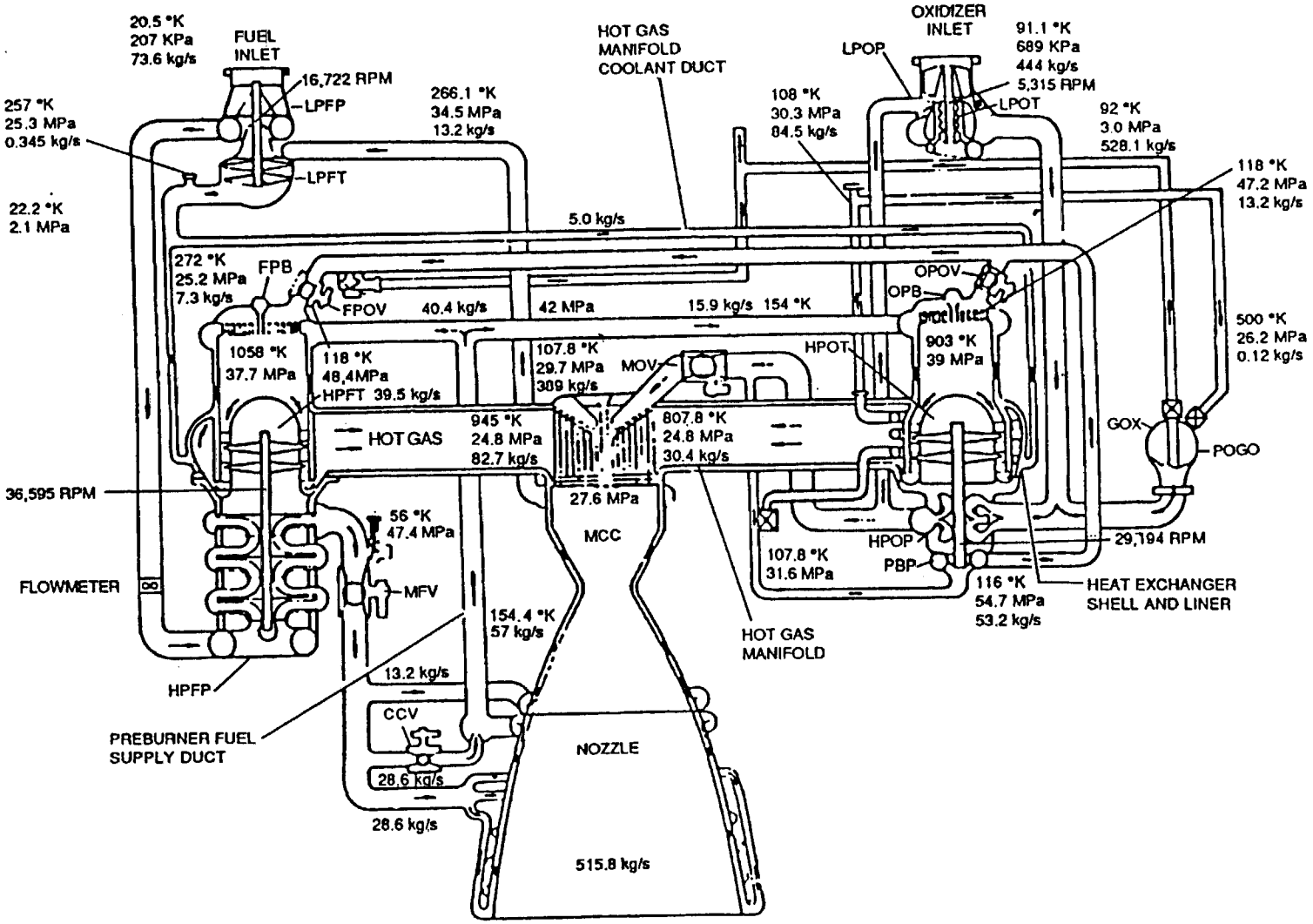

Figure 1. SSME Schematic with 109% Power Level Typical Operating Parameters.

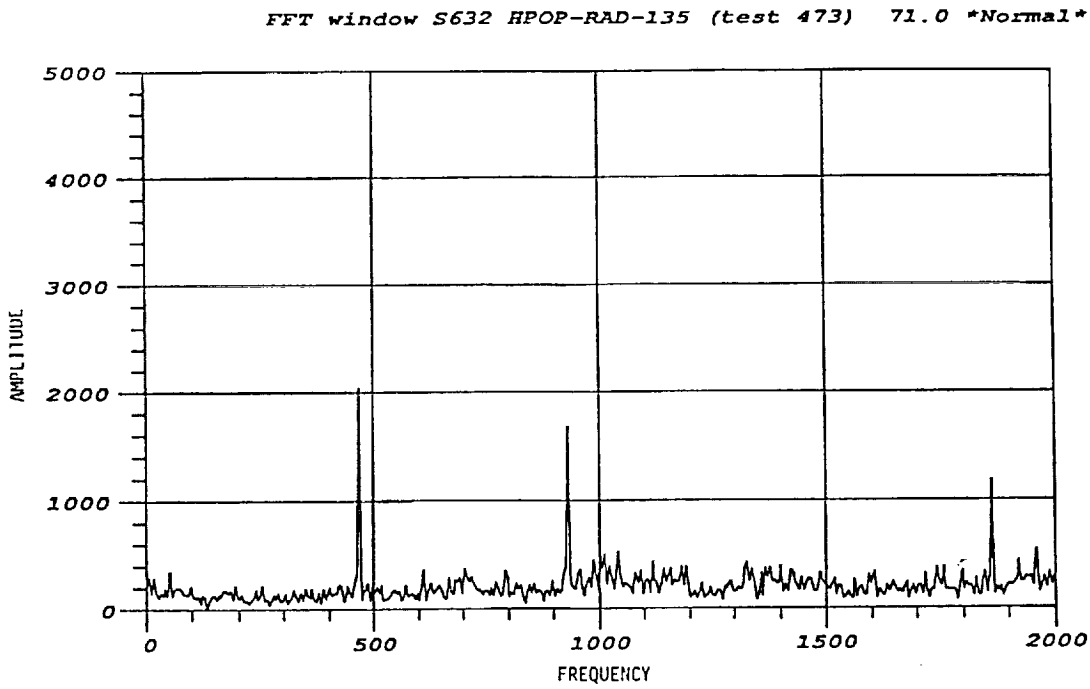

Figure 2. Typical Spectral Density vs Frequency of HPOP
(a) Normal Operation at t=71 sec.

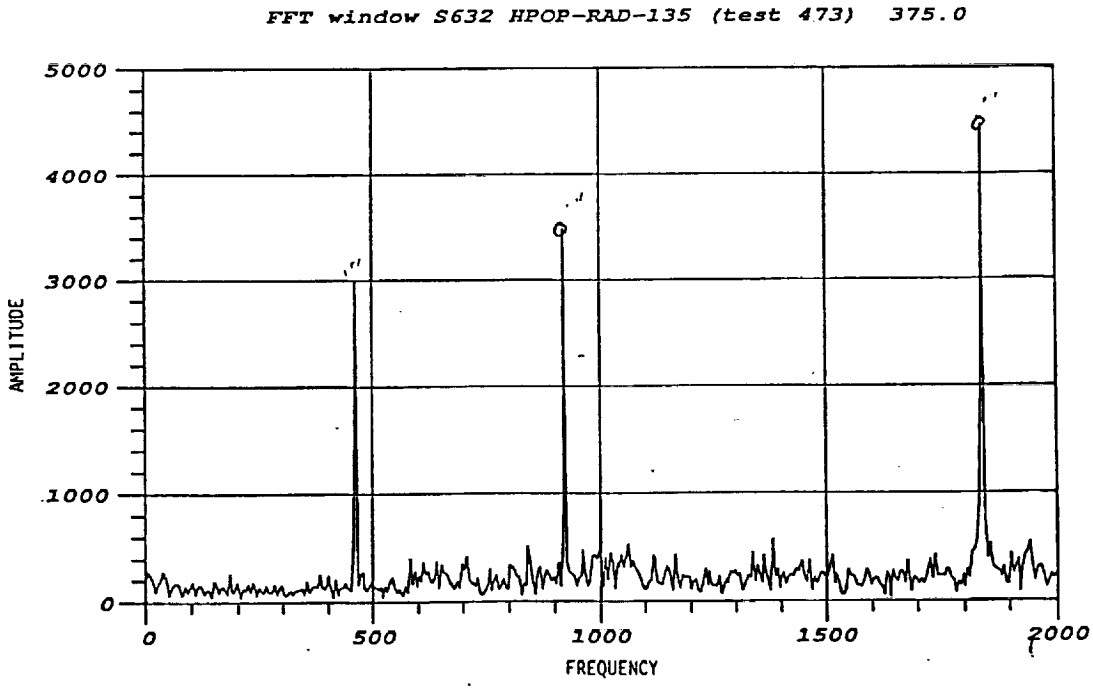

Figure 2. (cont.)
(b) Anomaly Condition at t=375 sec.

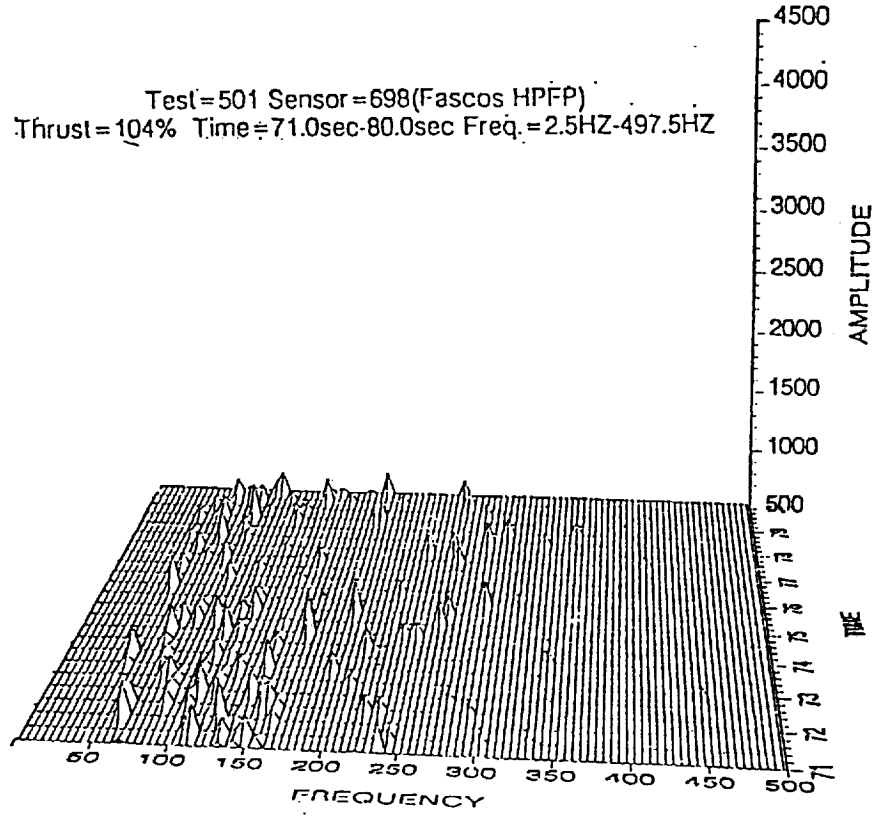

Figure 3. Cascade Plots of Spectral Density for HPFP
(a) Time from 71 sec. to 80 sec.

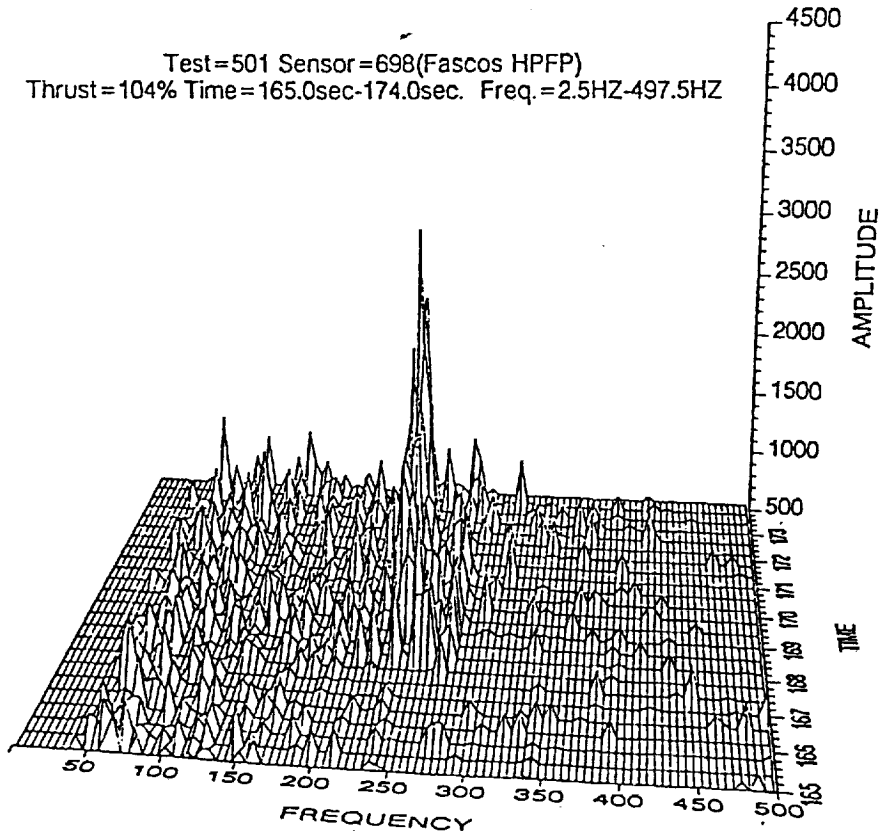

Figure 3. Cascade Plots of Spectral Density for HPFP
(b) Time from 165 sec. to 174 sec.

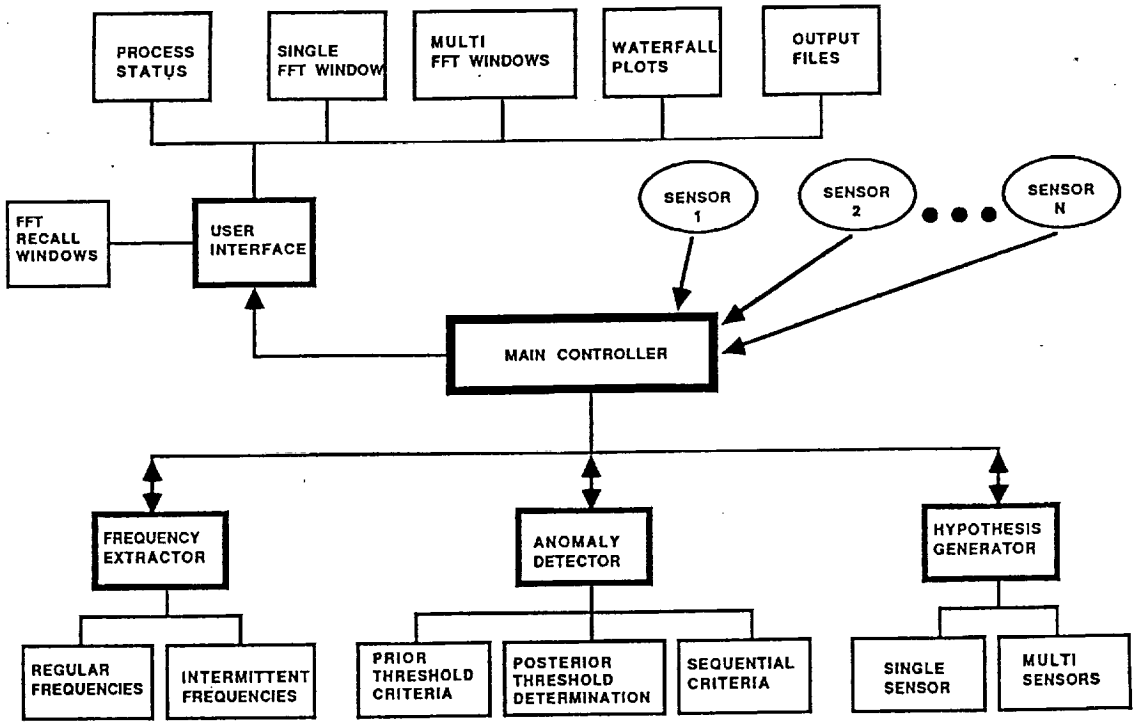

Figure 4. Architecture Structure of the Prototype Expert System for Automatic Detection of Anomalies in SSME.

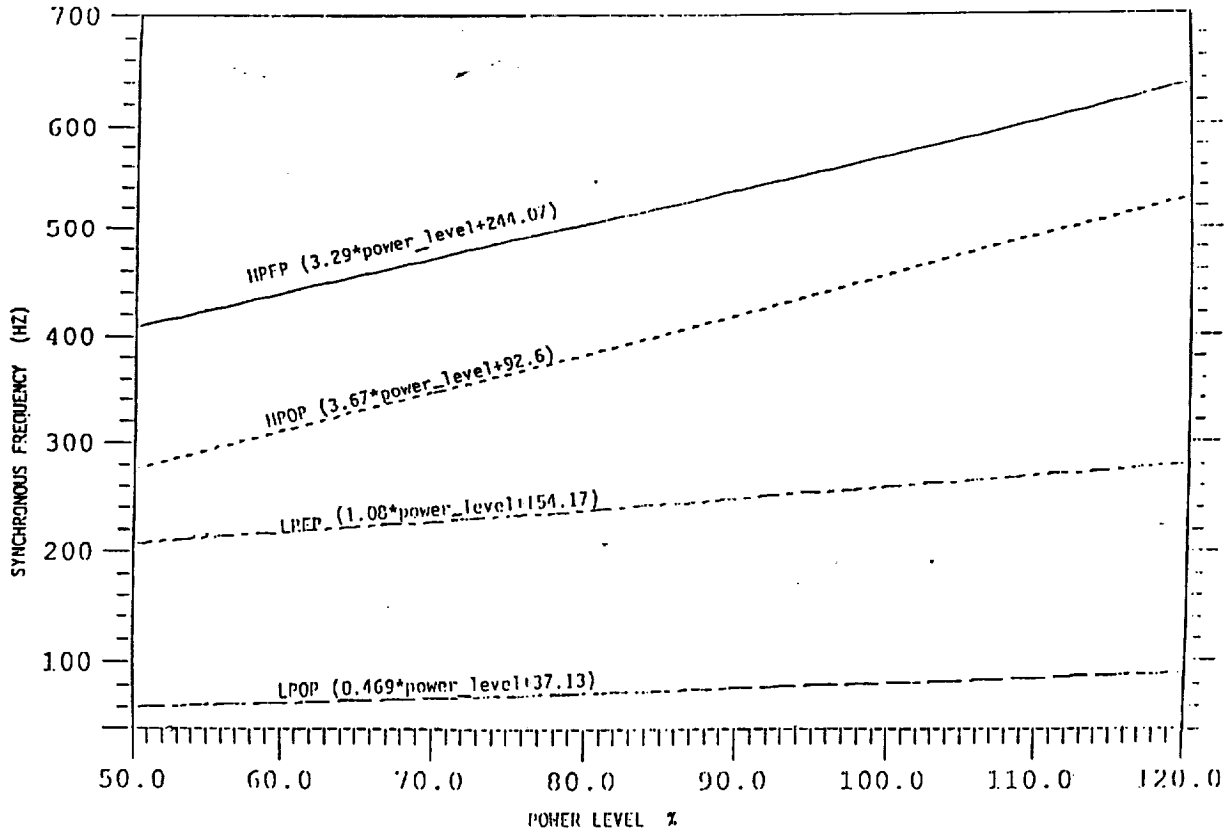

Figure 5. Empirical Functions of Sync. Frequency vs Power Level for Various Pumps.

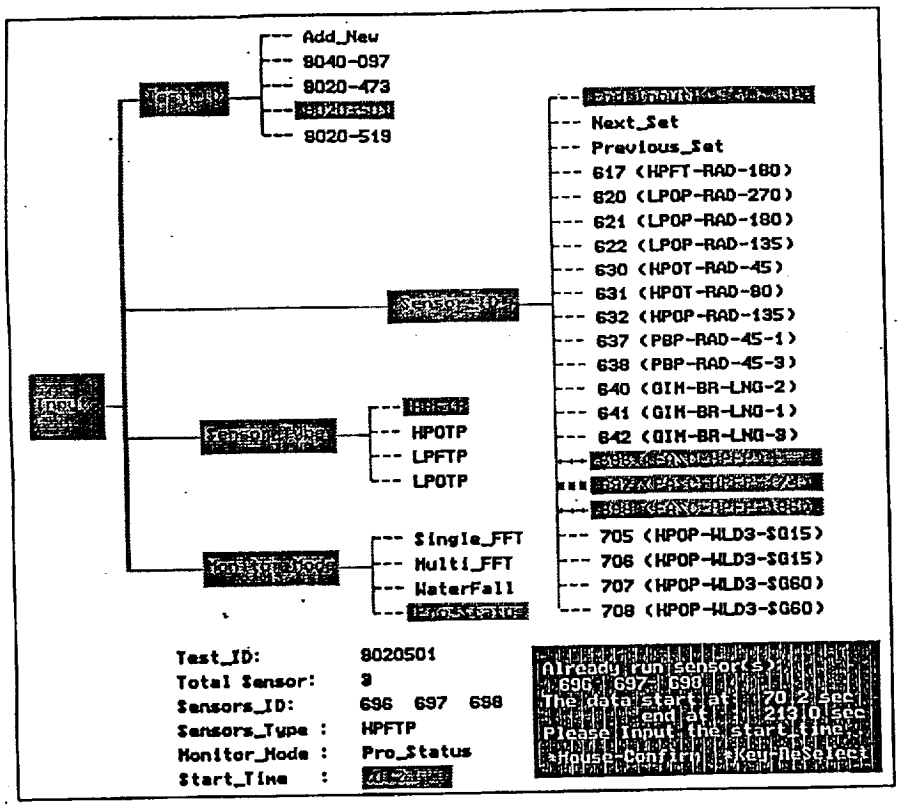

Figure 6. Interactive Session Windows
6a. Setup Processing Parameters

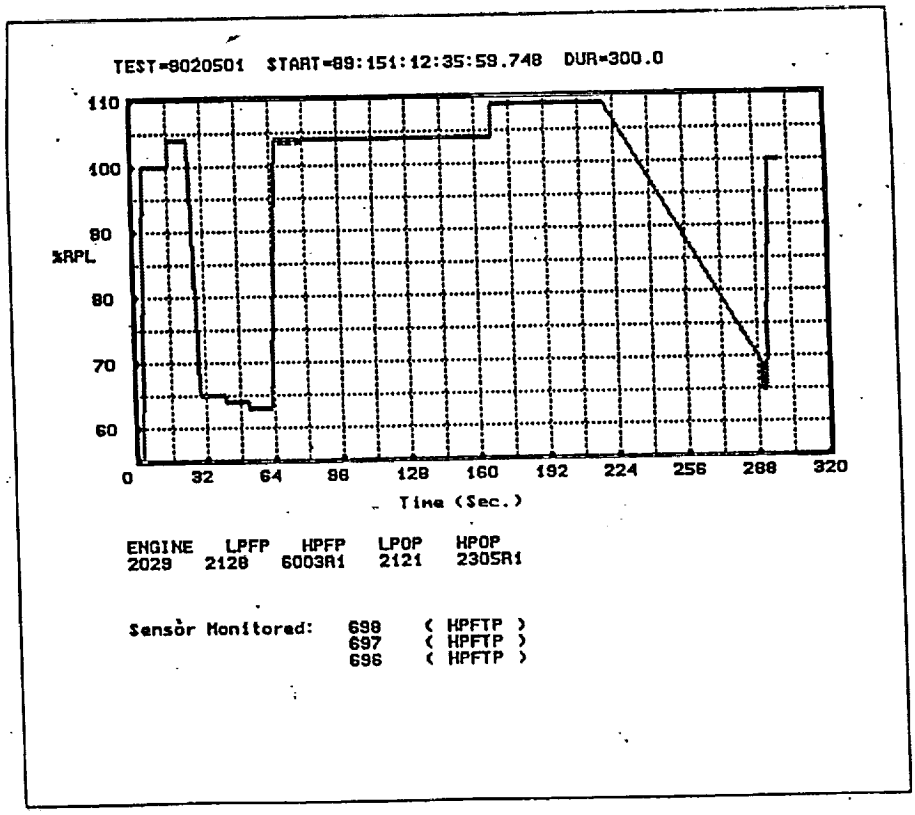

Figure 6. (cont.)
6b. Process Status: Power-level vs Time

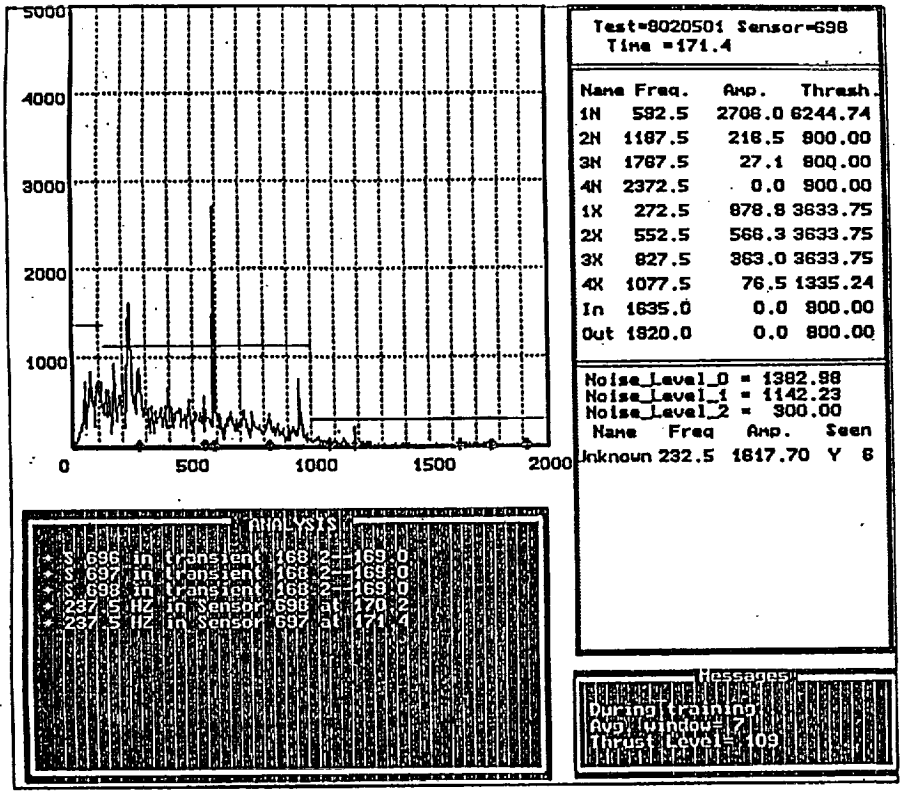

Figure 6. (cont.)
6c. Single FFT Plot & Analysis Message

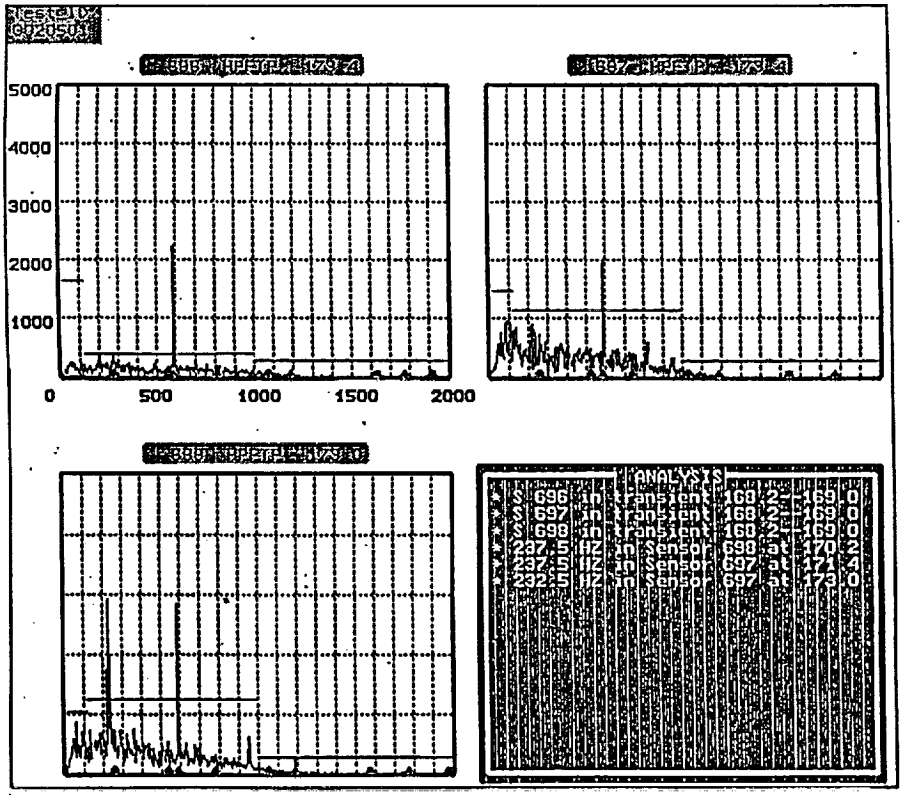

Figure 6. (cont.)
6d. Multiple FFT Plots & Analysis Message for Three Sensors

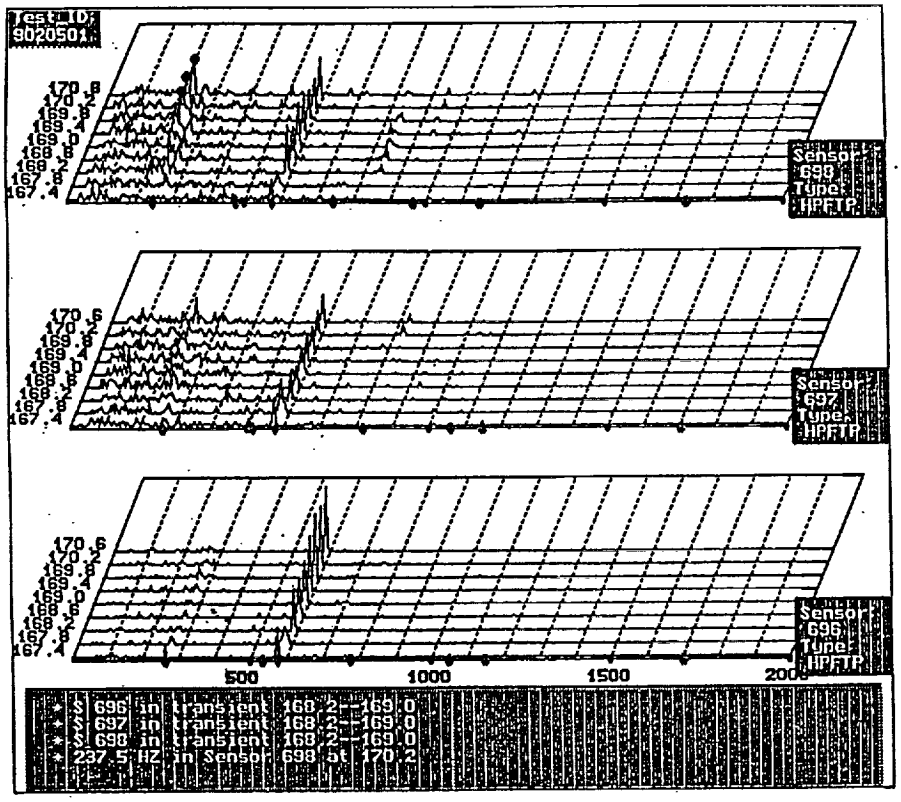

Figure 6. (cont.)
6e. Cascade Plots of Three Sensors

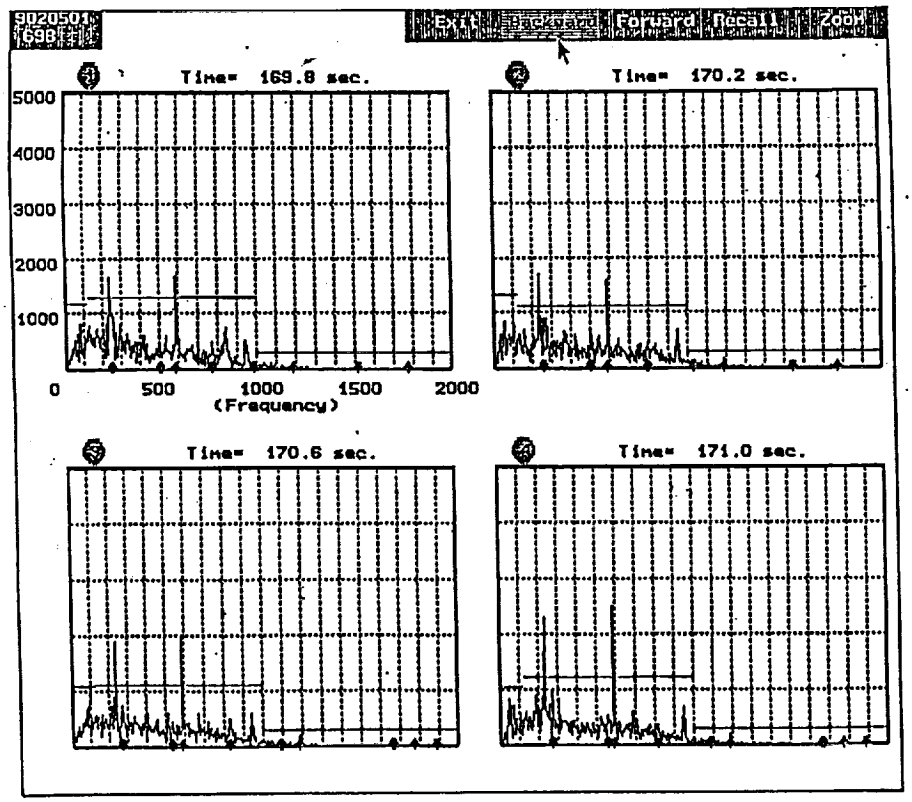

Figure 6 (cont.)
6f. FFT Windows for Post-test Analysis

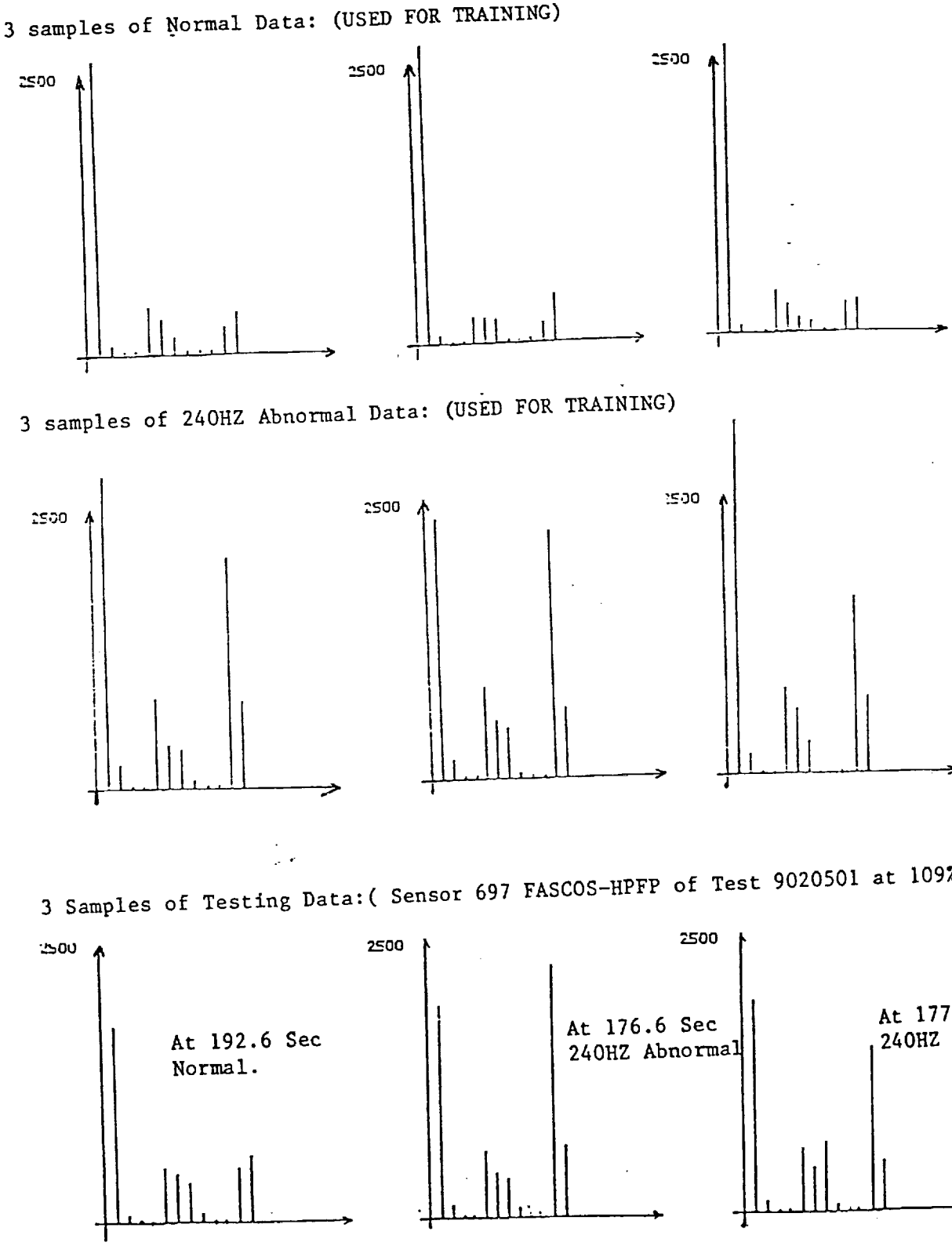

Figure 7. Samples of Normal and 240-hz Abnormal Data from HPFTP Sensors of Test 902-501 at the Thrust-level 109%.

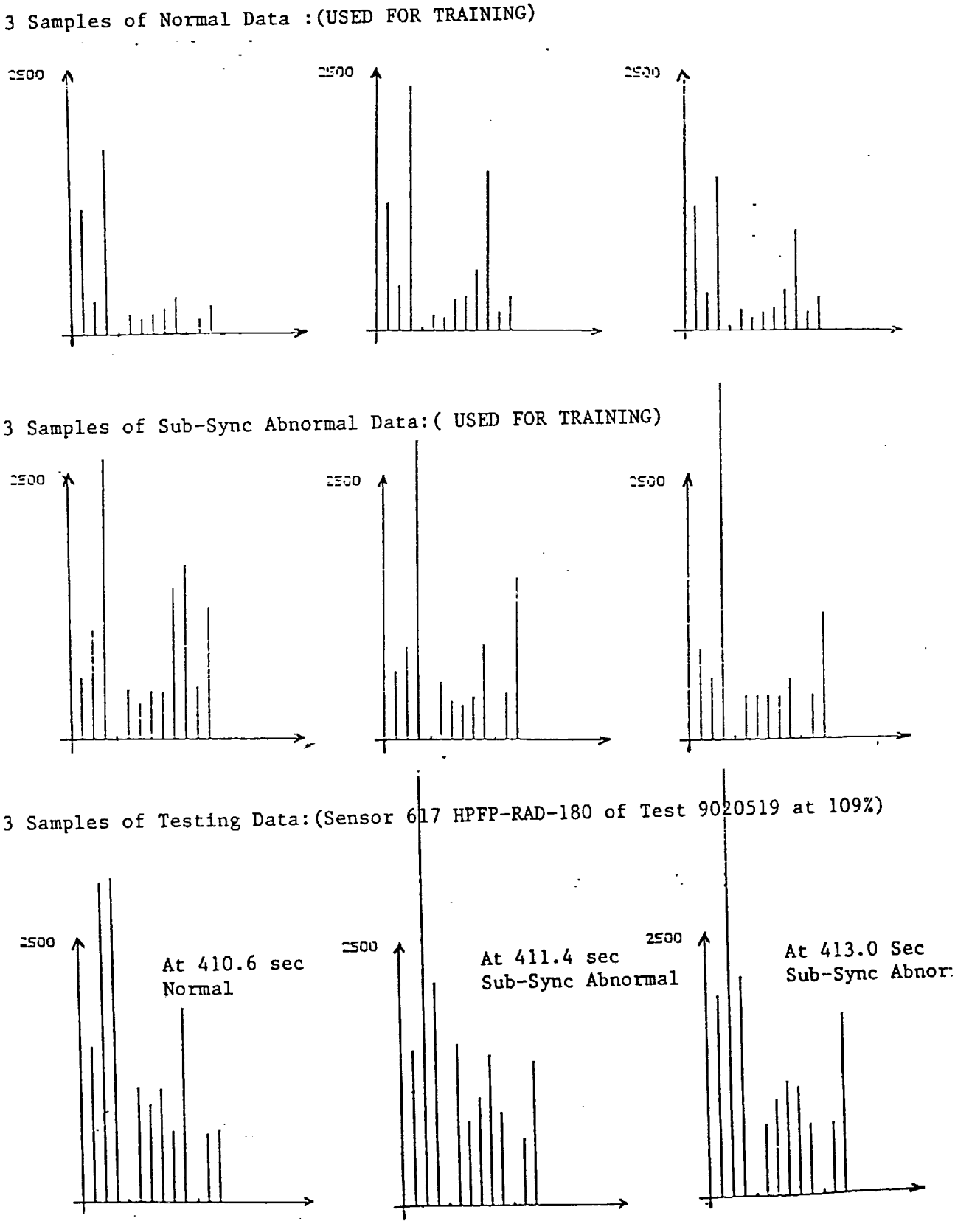

Figure 8. Samples of Normal and Sub-synchronous Abnormal Data from HPFTP Sensors of Test 902-519 at the Thrust-level 109%.

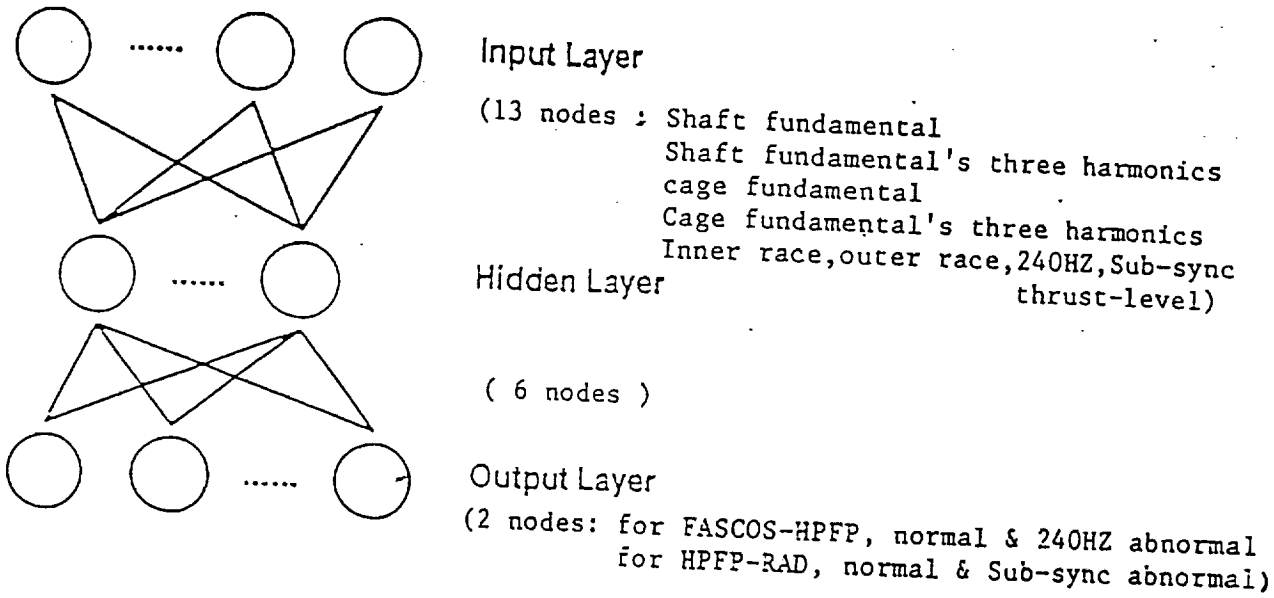

Figure 9. Three-layer Back-propagation Neural Network Architecture.

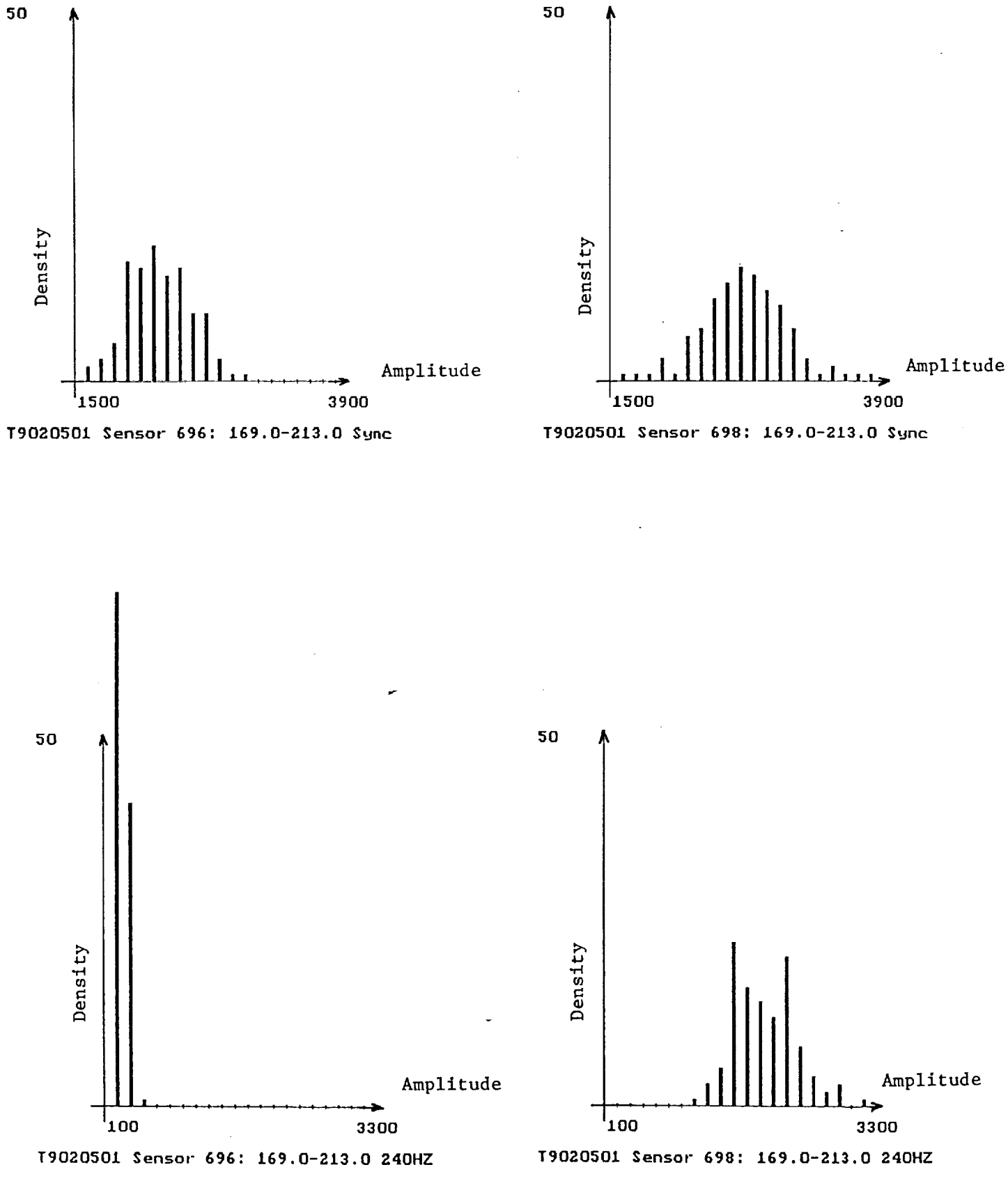

Figure 10. Data Histogram of Synchronous Frequency and 240-hz Frequency from Sensors 696 and 698.

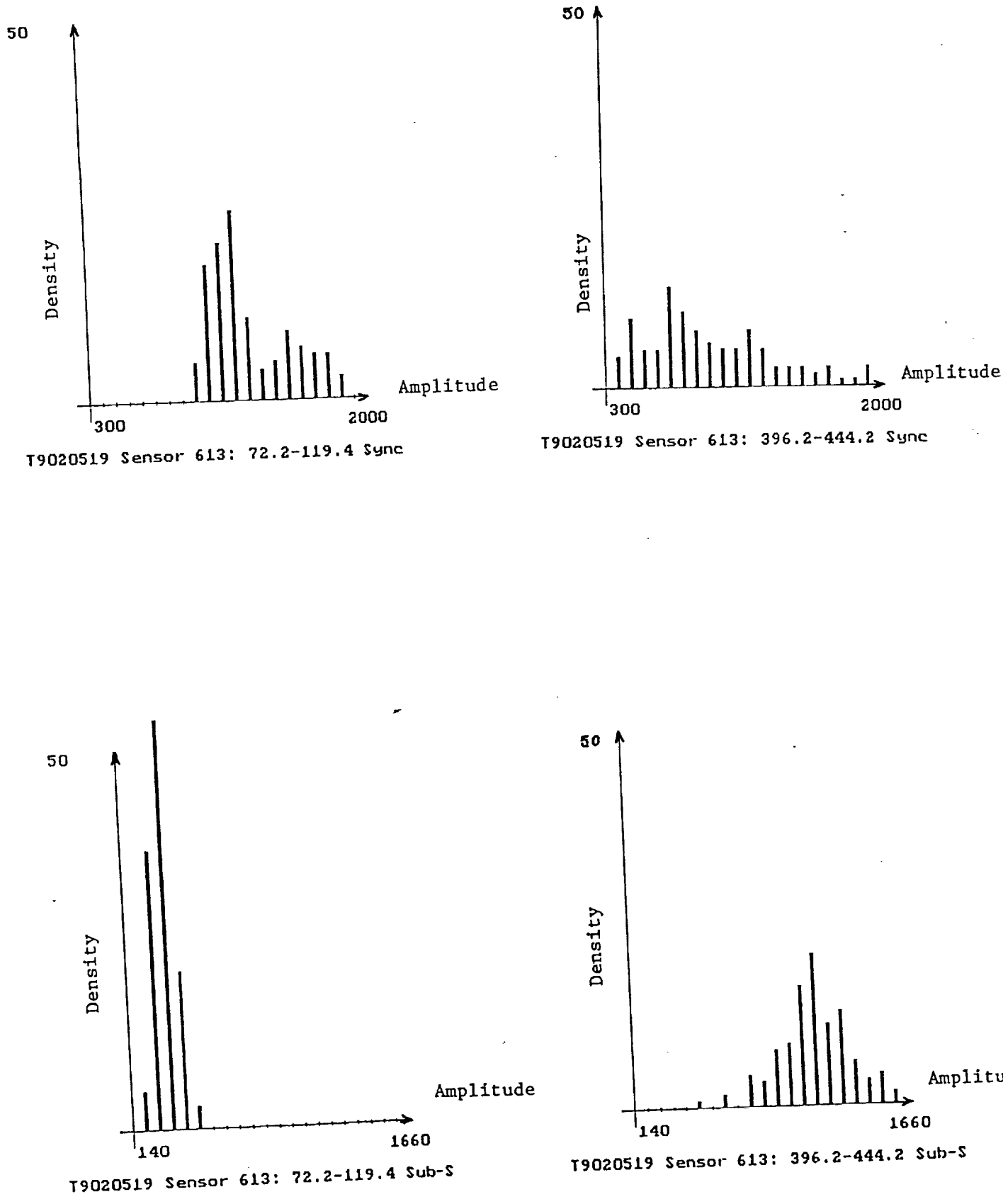

Figure 11. Data Histogram of Synchronous Frequency and Sub-synchronous Frequency from Sensor 613.

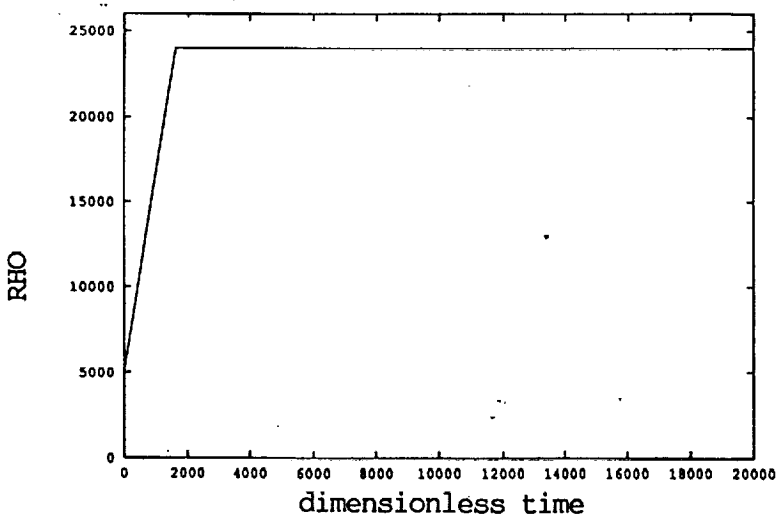

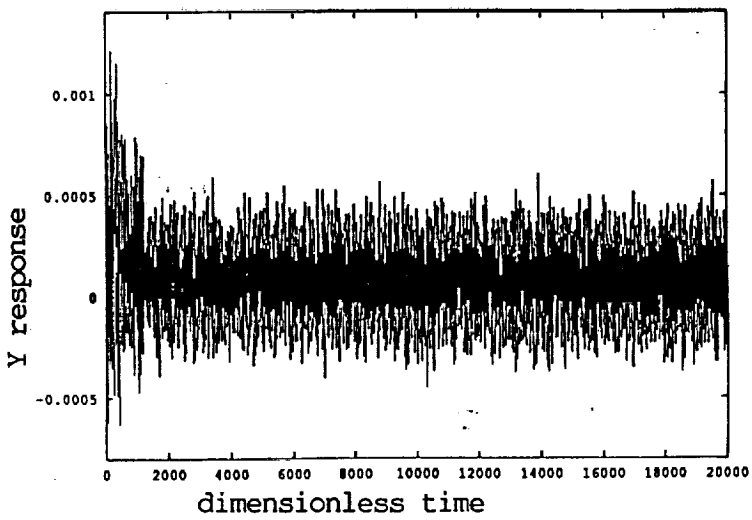

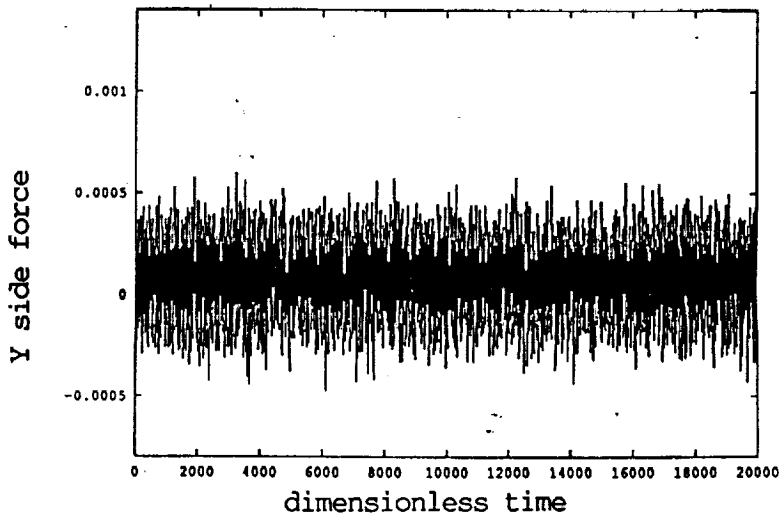

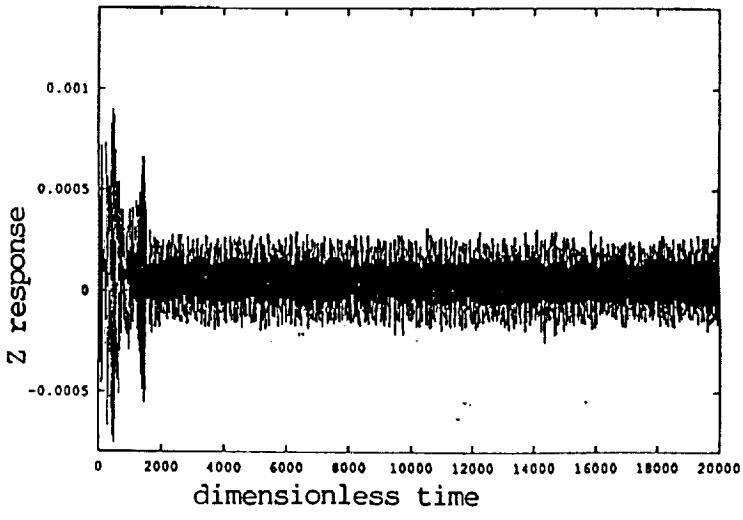

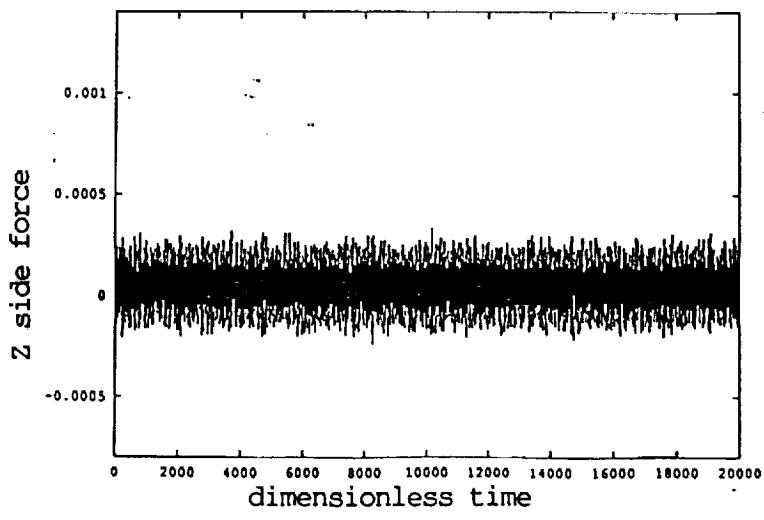

Figure 12. Sample Data Received on Nov. 15, 1992 (ROTOR.DB).

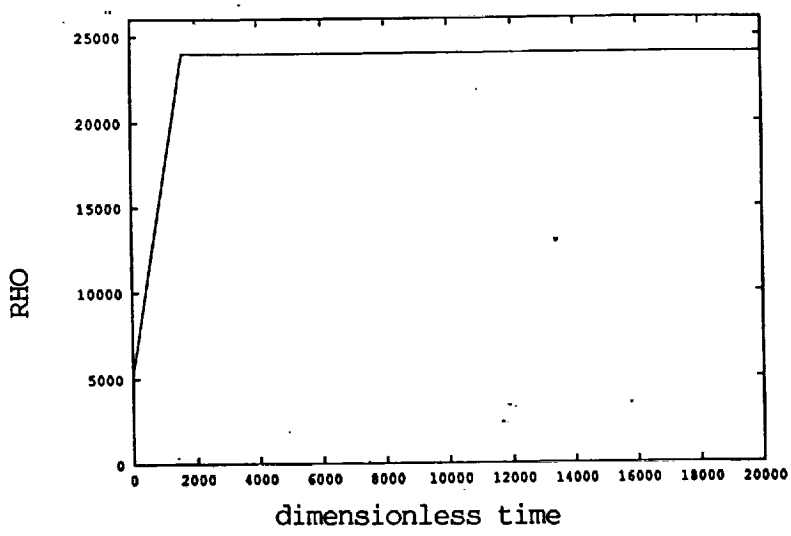

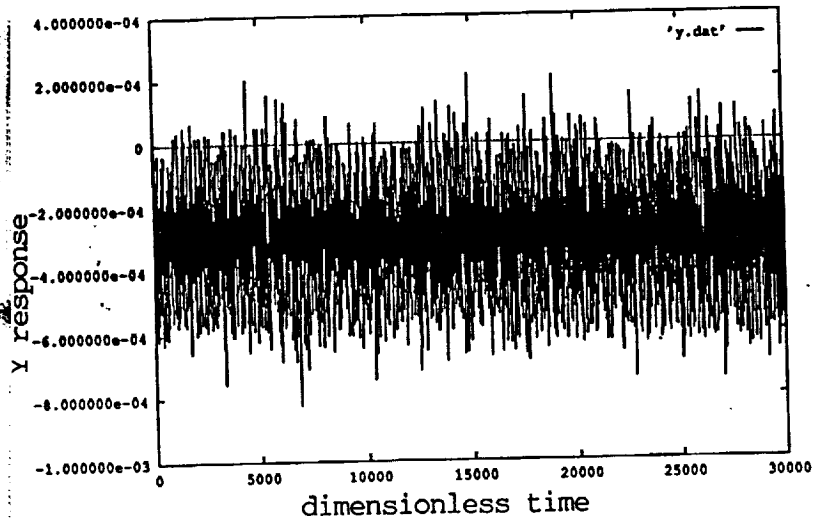

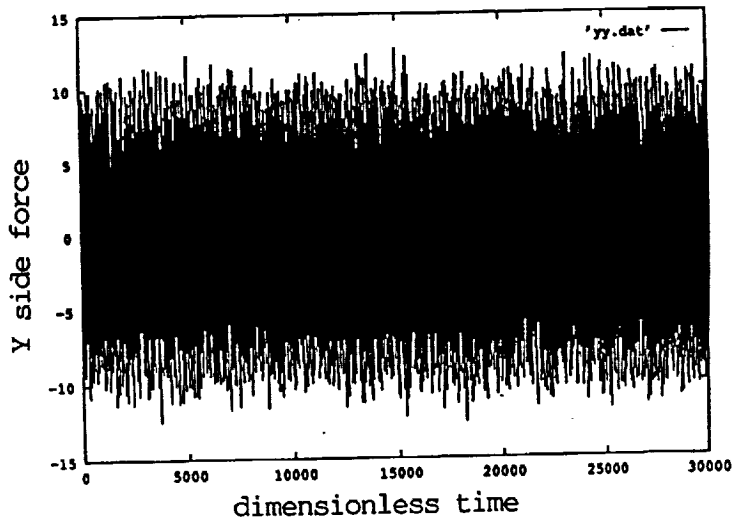

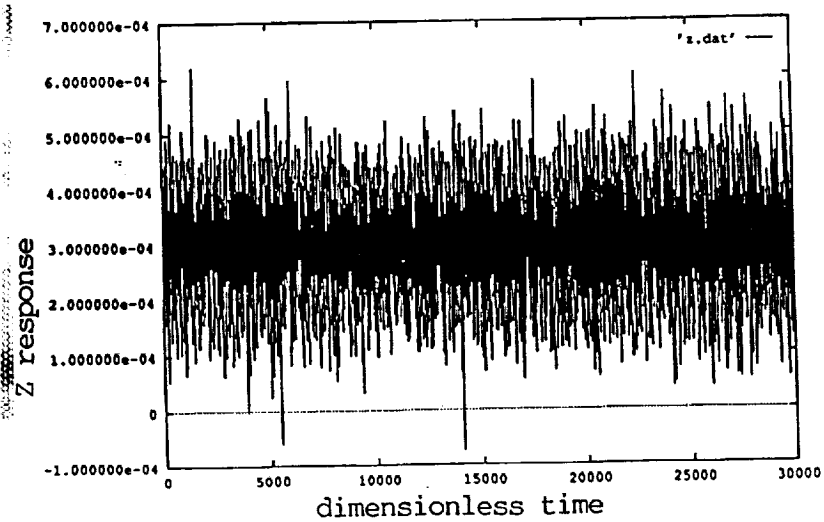

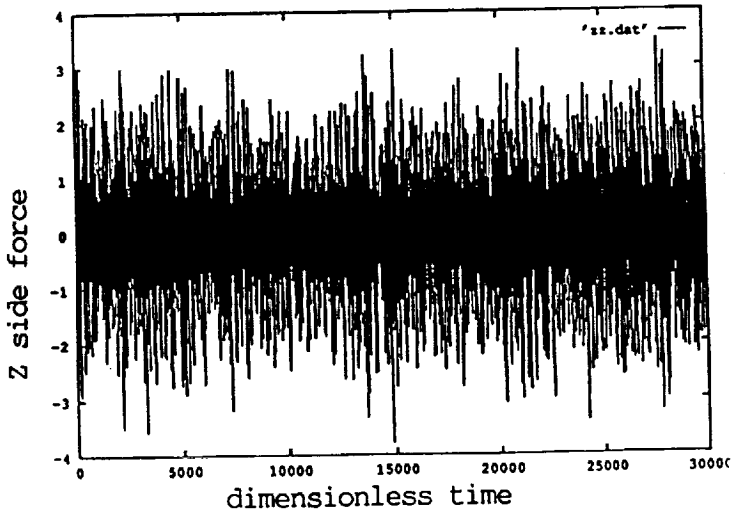

Figure 13. Sample Data Received on Feb. 18, 1993 (ROTOR.DB).

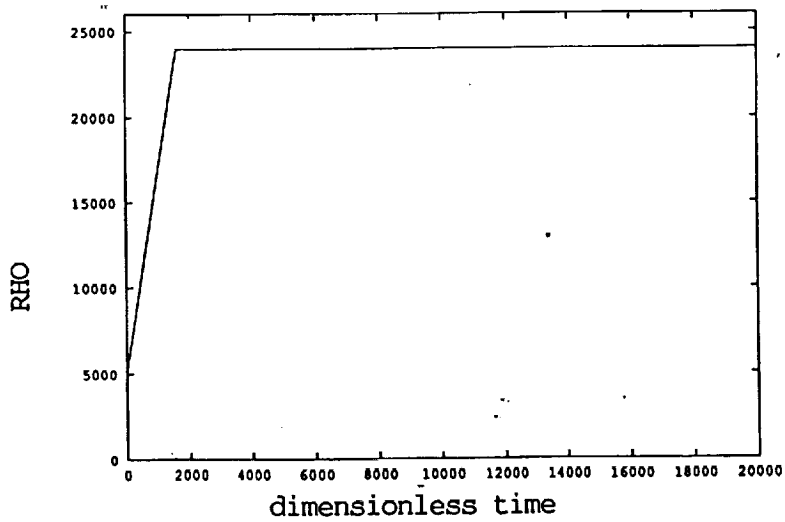

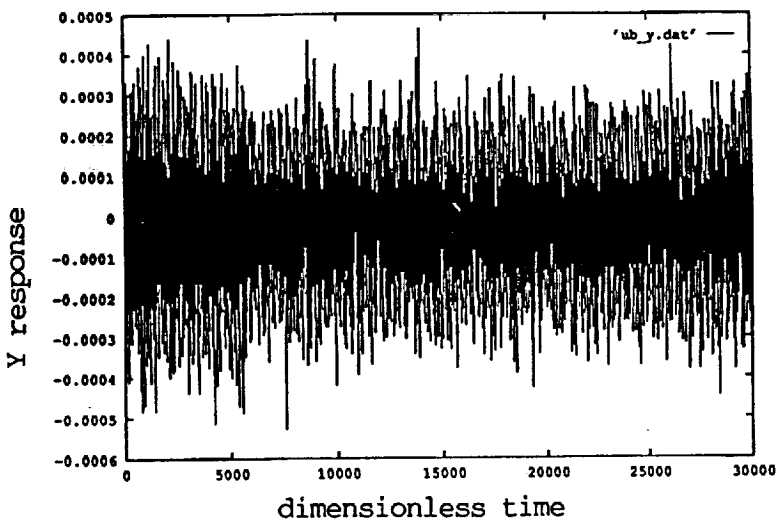

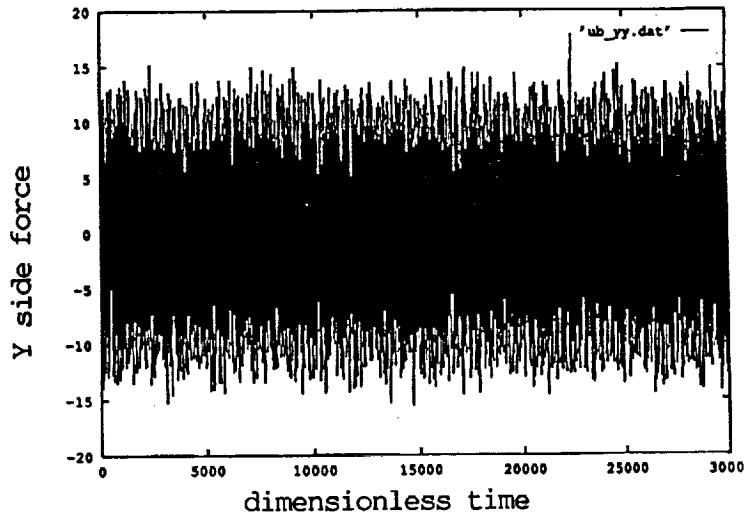

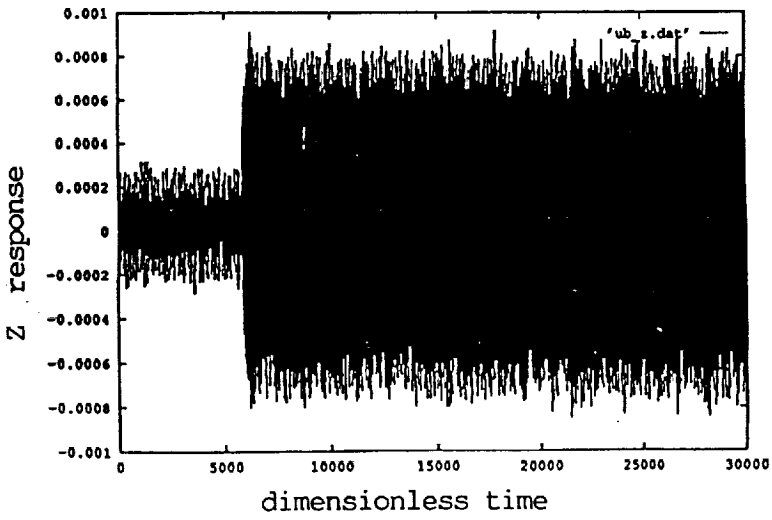

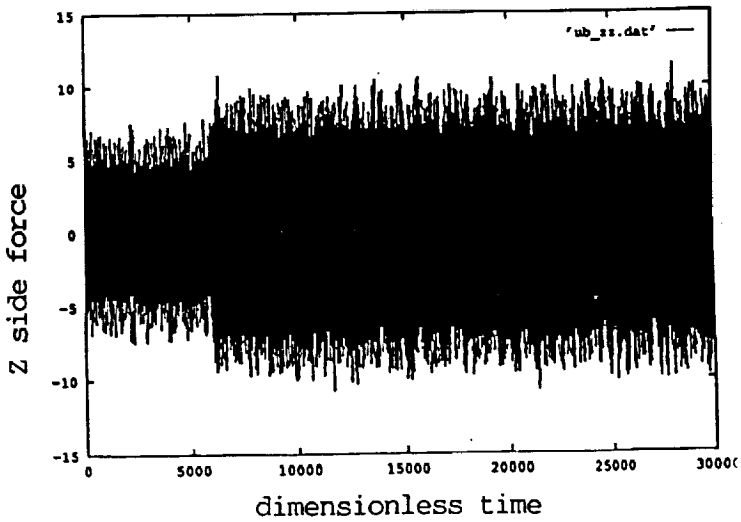

Figure 14. Sample Data Received on Feb. 18, 1993 (ROTOR.UB).

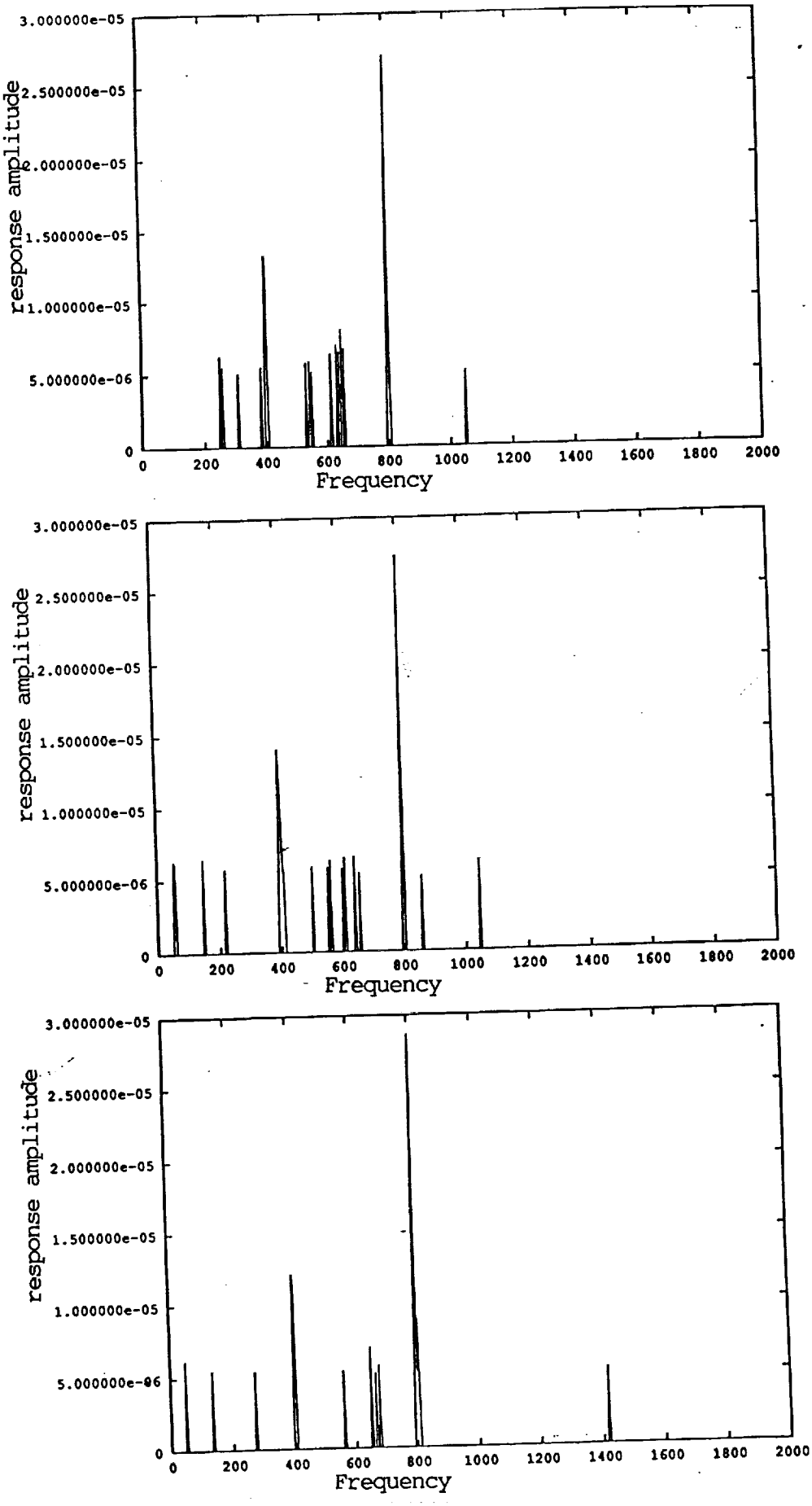

Figure 15. Response Amplitude After Frequency Extraction from Sample Data Received on Nov. 15, 1992 (ROTOR.DB).

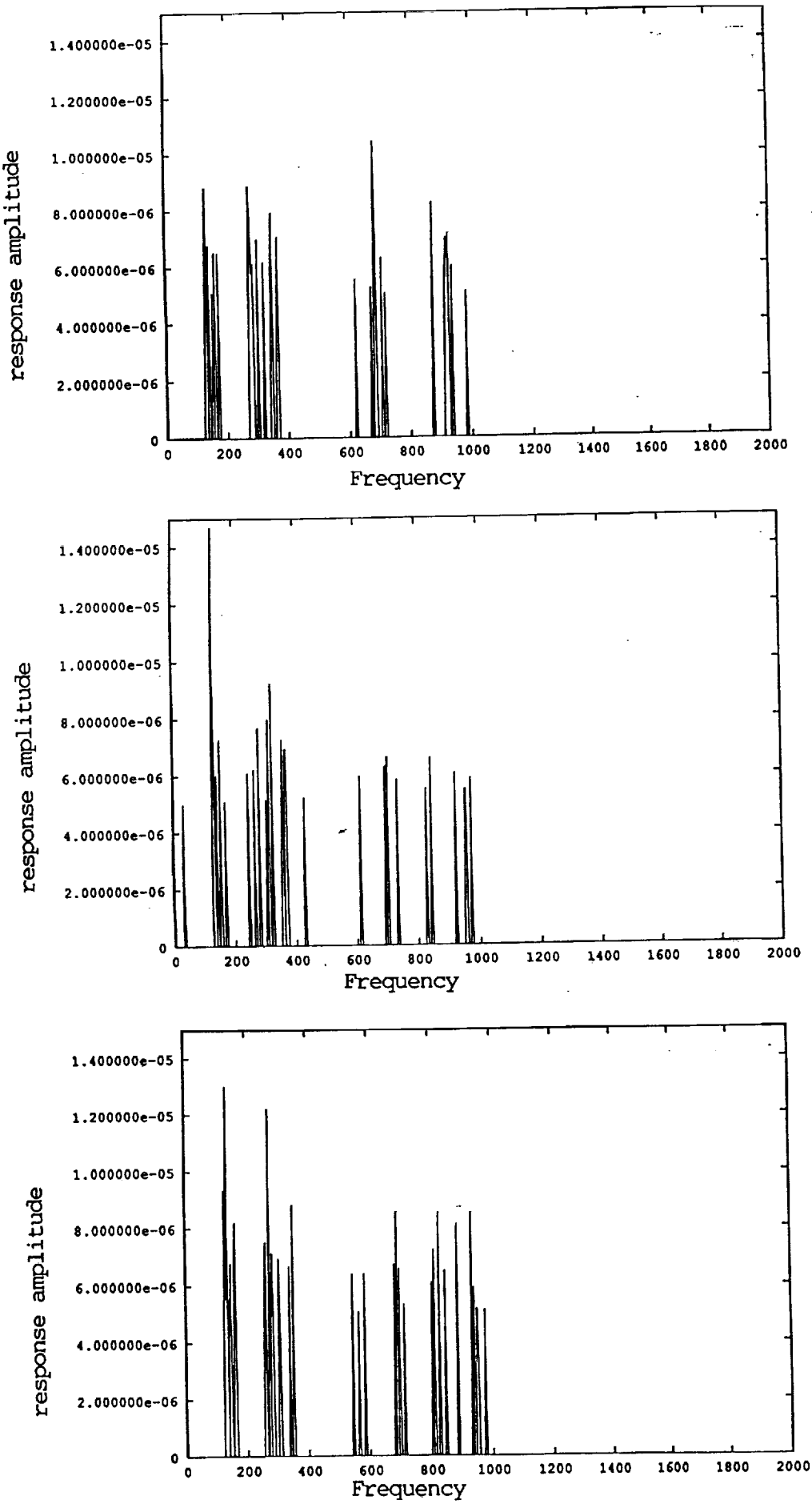

Figure 16. Response Amplitude After Frequency Extraction from Sample Data Received on Feb. 18, 1993 (ROTOR.DB).

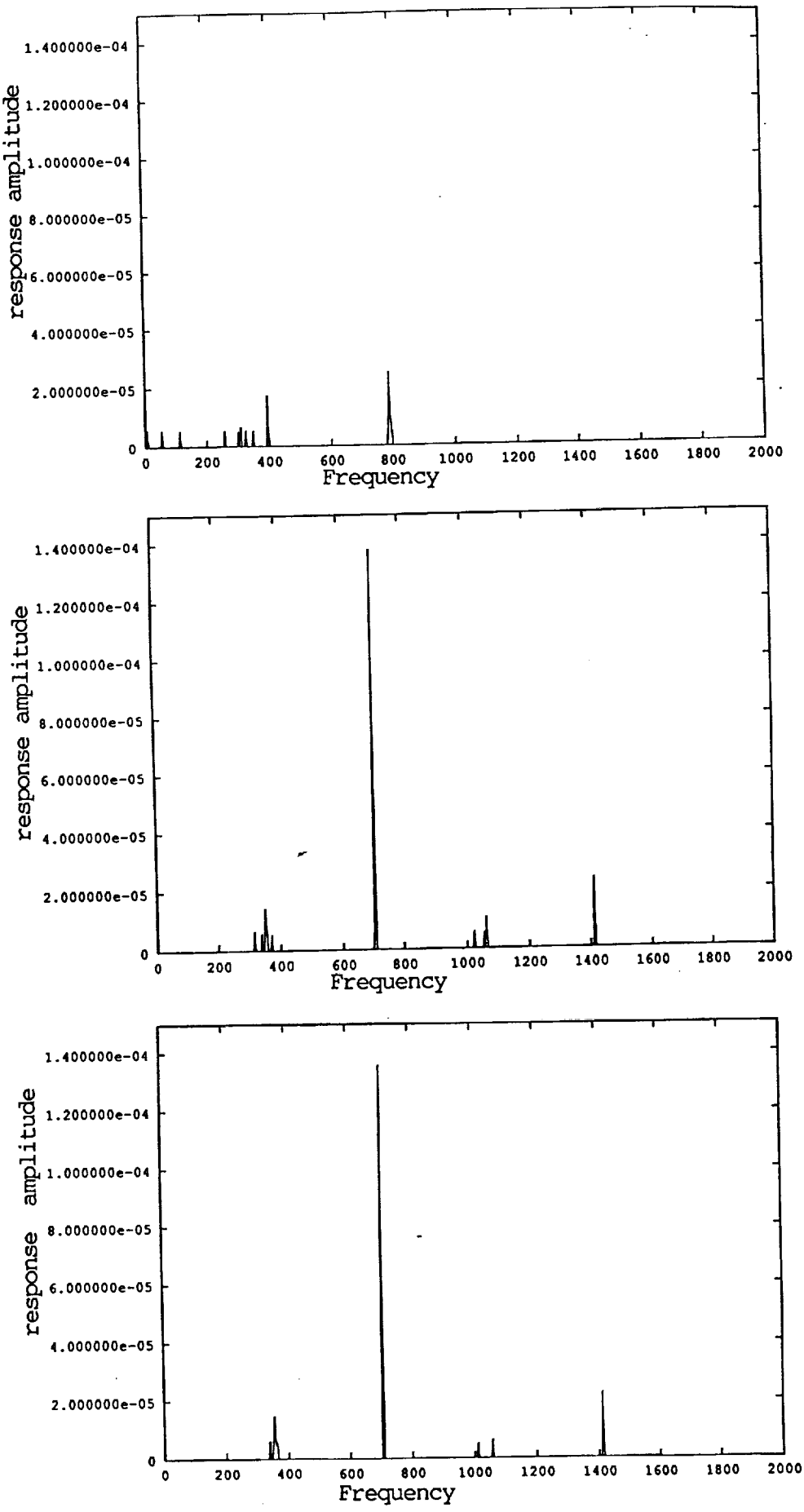

Figure 17. Response Amplitude After Frequency Extraction from Sample Data Received on Feb. 18, 1993 (ROTOR.UB).

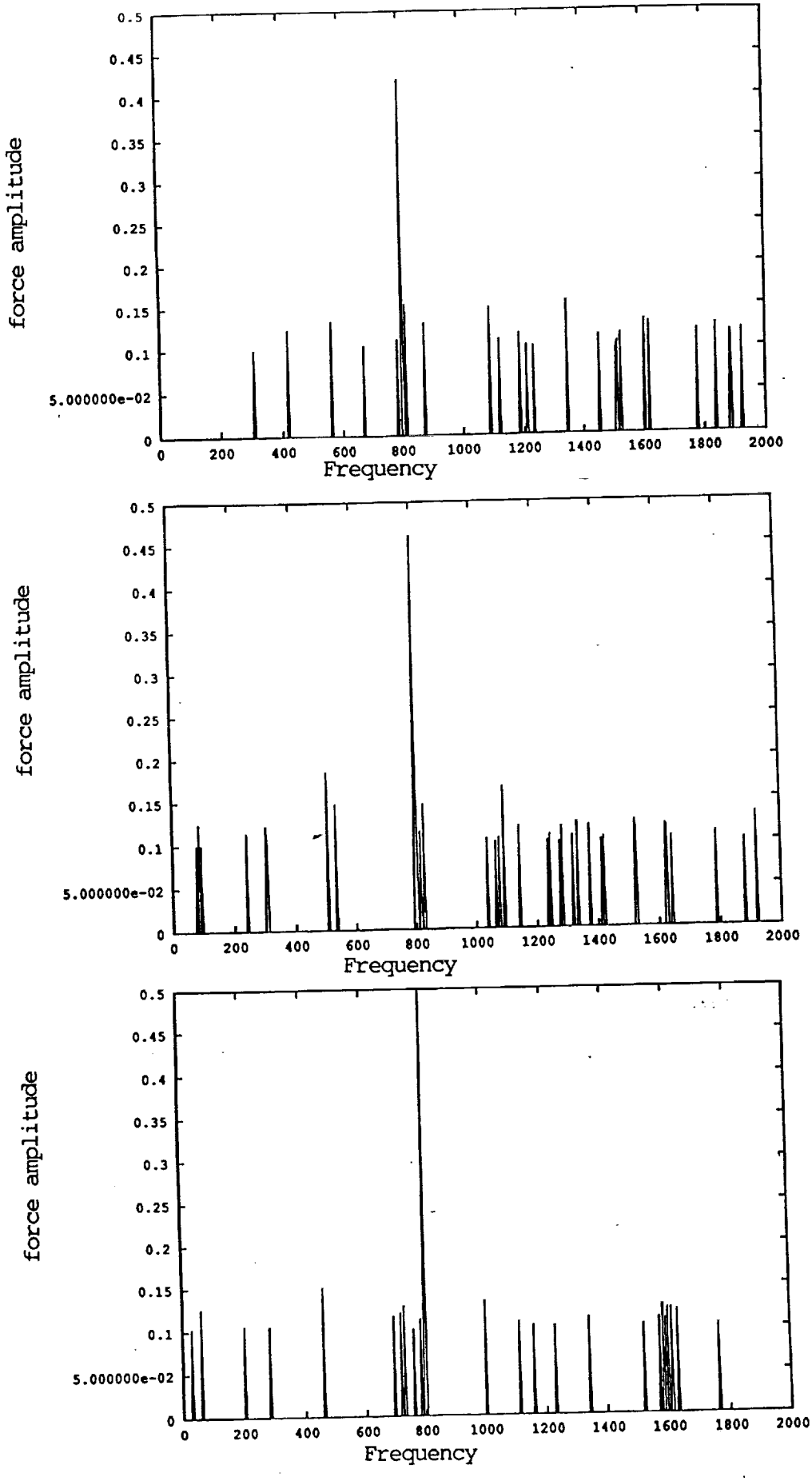

Figure 18. Force Amplitude After Frequency Extraction from Sample Data Received on Nov. 15, 1992 (ROTOR.DB).

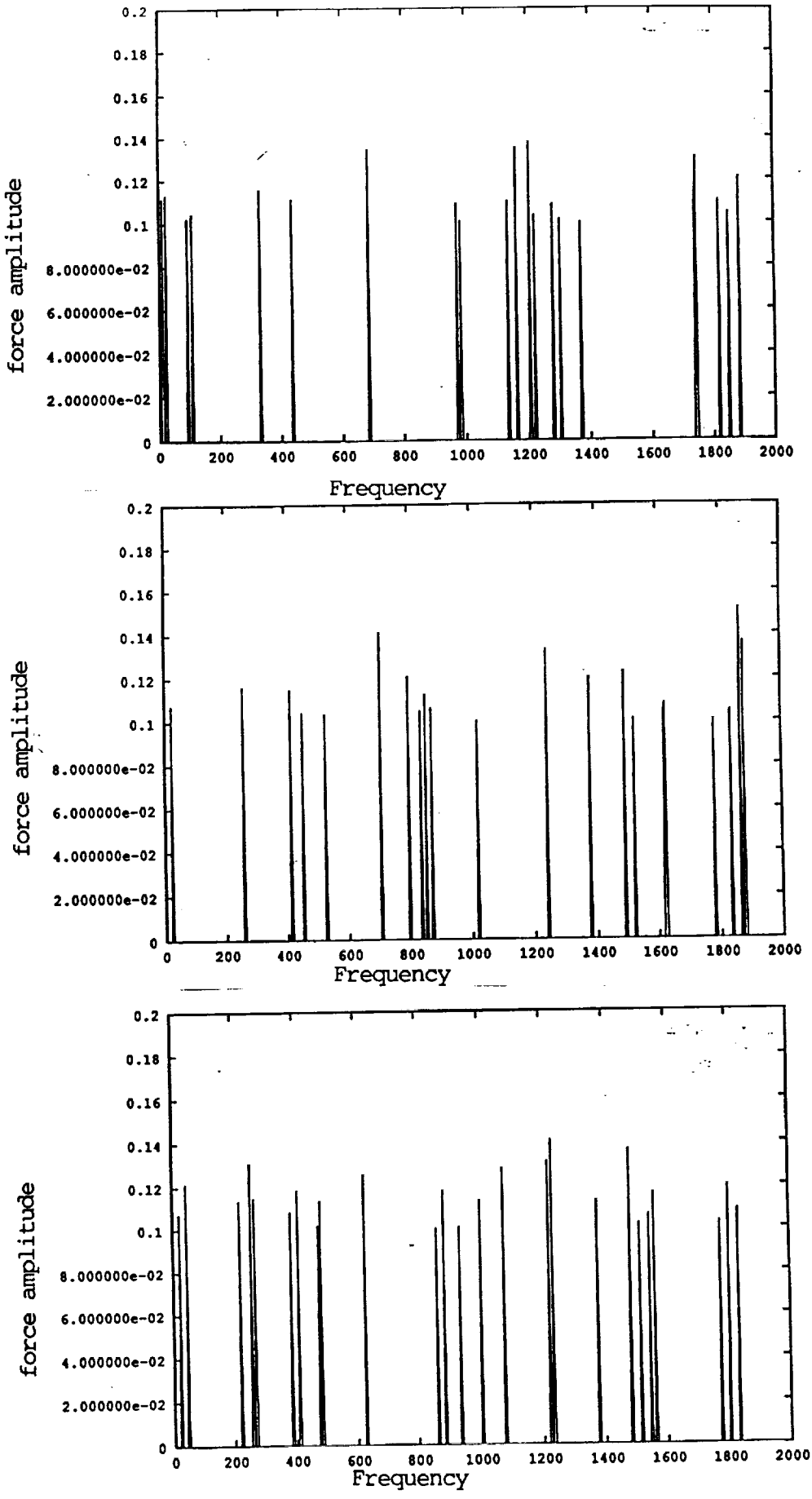

Figure 19. Force Amplitude After Frequency Extraction from Sample Data Received on Feb. 18, 1993 (ROTOR.DB).

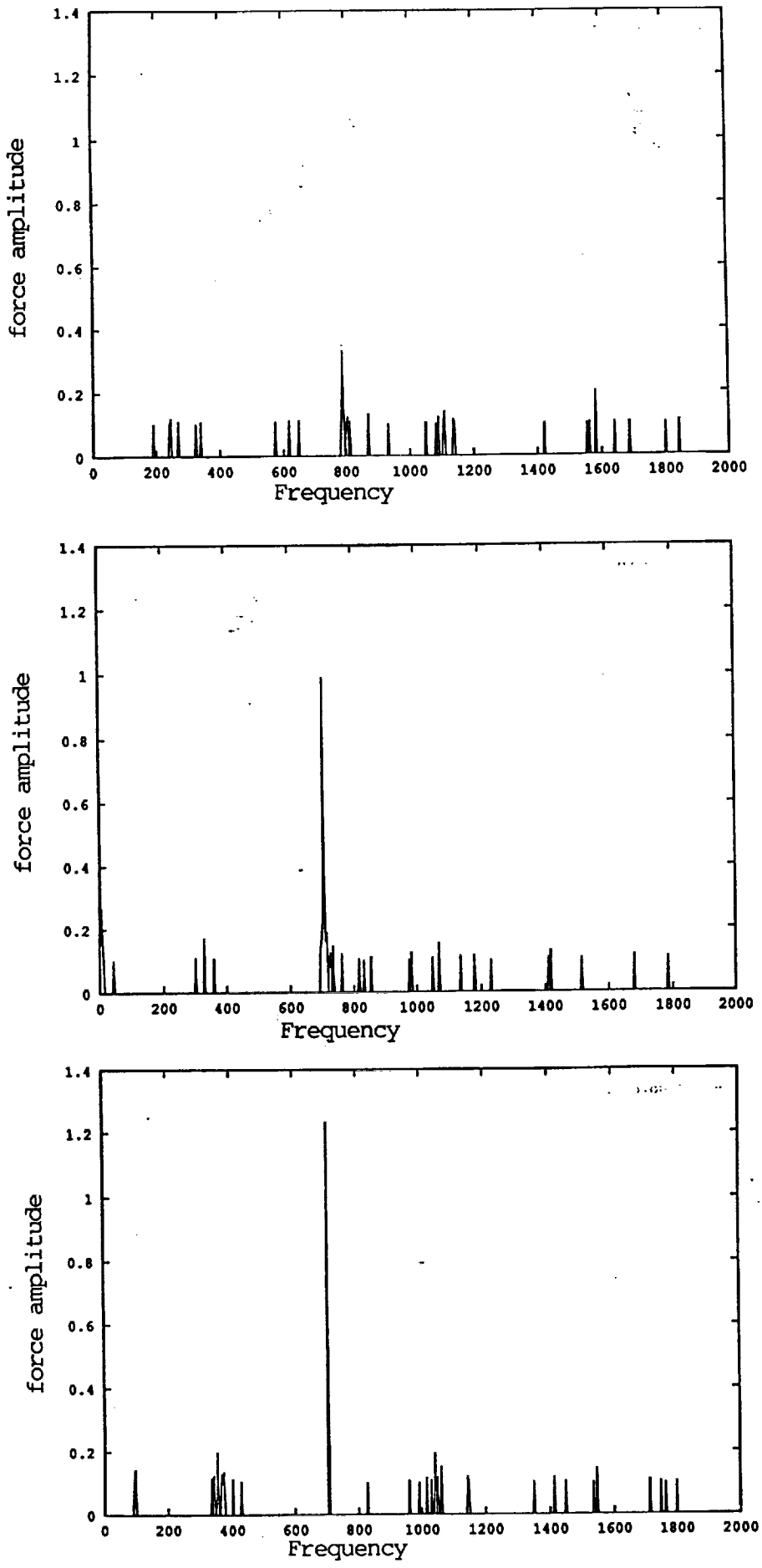

Figure 20. Force Amplitude After Frequency Extraction from Sample Data Received on Feb. 18, 1993 (ROTOR.UB).

902-097	
NASA's REPORT	PRESENT RESULTS
LOX SIDE OBSERVATIONS * HPOTP: 2X CAGE PRESENT IN ACCEL DATA AT 104% & 109%RPL(0.4 Grms MAX.). CAGE RATIO CONSISTENT THROUGH TEST AT -0.434	2X cage does appear in Sensor 637 (PBP-RAD-45-1) and 638(PBP-RAD-45-3) around 160.0 sec.,but system can not detect them now. *Analysis*: Maybe 5 std. is too high and these 2X cages don't show in more than 3 consecutive windows.
FUEL SIDE OBSERVATIONS * HPFTP: ANOM. FREQ. 1750-1800 HZ (10 Grms MAX). ANOM. FREQ. 560-600 HZ(7 Grms MAX)	Anom. Freq. 1750-1830 HZ presents in FASCOS-HPFP Sensors(696,697,698) around 97.0 sec..
* LPFTP: "330HZ" ACTIVITY ALONG WITH "330HZ" LPFTP SYNC. MODULATION SIDEBANDS. LPFP-RAD-240 ACCEL BAD (E/S +220 SEC.)	310HZ appears in Sensor 603(LPFT-RAD-180) at 393.4 sec..

TABLE 1

902-501	
NASA's REPORT	PRESENT RESULTS
LOX SIDE OBSERVATIONS * HPOTP: PASS ALL GREENRUN CRITERIA; NO ANOMALIES PRESENT.	No anomalies present in HPOP-WLD3 Sensors(705,706,707,708) and ES6740 sensors(520,522).
FUEL SIDE OBSERVATIONS * HPFTP: ANOM. FREQ.'s PRESENT AT 109% AT 240HZ and 950HZ(MAX.AMP.1.9 Grms and 1.5 Grms RESPECTIVELY).ANOMALIES ARE MODULATING ABOUT SYNC.. PASSES ALL GREEN RUN CRITERIA.	Sensor 697(FASCOS-HPFP) and Sensor 698(FASCOS-HPFP) present Anom. Freq. 's at 109% at 240HZ around 171.0sec. , but no 950HZ shows ANOM. in FASCOS sensors (696,697,698).
* LPFTP: 330HZ APPEARS TO COALESCE WITH SYNC. CAUSING GREEN RUN SPEC. VIOLATION SYNC..	300HZ appears in Sensor 603(LPFT-RAD-180) at 91.4 sec..

TABLE 2

902-519	
NASA's REPORT	PRESENT RESULTS
LOX SIDE OBSERVATIONS * HPOTP: PASS ALL GREENRUN CRITERIA; ACCEPTABLE FOR FLIGHT.	NO ANOMALIES PRESENT IN PBP-RAD Sensors(637,638).
* LPOTP: ANOMALY PRESENT BETWEEN 800-900 HZ.	We don't have any LPOTP sensors.
FUEL SIDE OBSERVATIONS * HPFTP: 50% SUBSYNC. PRESENT @109% (MAX. AMP.-1.0Grams);POSSIBLY PRESENT @104%. FURTHER ANALYSIS NECESSARY.	System couldn't detect 50% subsync. *Analysis*: Lowering the 5 std. to 3 std. and dividing the white noise into two levels may help. Further work needs to be done.
* HPFTP: HPFT RAD 180 HAS LARGE SPIKE.	Sensor 612(HPFP-RAD-180) shows large spike at 1730HZ at 141.0 sec.. Sensor 617(HPFT-RAD-180) shows large spike at 5HZ at 91.4 sec...
* LPFTP: 330HZ PRESENT AT 104% & 109% MAX. AMP. 4.0 Grams FEEDS THRIUGH TO ALL TURBOPUMPS.	We don't have any LPFTP sensors.

TABLE 3

902-473	
NASA's REPORT	PRESENT RESULTS
LOX SIDE OBSERVATIONS * SYNCHRONOUS RUNNING ON HIGH SIDE AT 100% PWL 450 HZ	PBP sensors(635,636,637,638) show Anomalies of Synchronous (462.5HZ) around 360.0 sec..
FUEL SIDE OBSERVATIONS * PSEUDO 3N AT 1725 HZ COINCIDES WITH 3N AT S +70 SEC	We don't have any FUEL SIDE sensors.

TABLE 4

Raw Data (Y-Response of ROTOR.UB, Received on Feb 18,1993)
After 300 training cycles
Random Selection of Training Data Sets

Self-Testing After Training

Actual Class of Observation

	Normal	Abnormal	Total	P2%
Normal	3	0	3	100
Abnormal	0	5	5	100
Total	3	5	8	100
P1%	100	100	100	100

New Data Testing After Training

Actual Class of Observation

	Normal	Abnormal	Total	P2%
Normal	1	0	1	100
Abnormal	1	5	6	83
Total	2	5	7	91
P1%	50	100	75	83

NOTE: P1: p(prediction=x, actual=x), P2: p(actual=x, prediction=x)

Table 5. Neural Networks Results of ROTOR.UB
a. for Y-Response

Raw Data (Y-Force of ROTOR.UB, Received on Feb 18,1993)
After 300 training cycles
Random Selection of Training Data Sets

Self-Testing After Training

Actual Class of Observation

	Normal	Abnormal	Total	P2%
Normal Abnormal	3 0	0 5	3 5	100 100
Total	3	5	8	100
P1%	100	100	100	100

New Data Testing After Training

Actual Class of Observation

	Normal	Abnormal	Total	P2%
Normal Abnormal	1 2	0 4	1 6	100 67
Total	3	4	7	84
P1%	33	100	67	75

NOTE: P1: p(prediction=x, actual=x), P2: p(actual=x, prediction=x)

Table 5. Neural Networks Results of ROTOR.UB
b. for Y-Force

Raw Data (Y-Response of ROTOR.DB, Received on Feb 18,1993)
After 300 training cycles
Random Selection of Training Data Sets

Self-Testing After Training

Actual Class of Observation

	Normal	Abnormal	Total	P2%
Normal	6	0	6	100
Abnormal	0	1	1	100
Total	6	1	7	100
P1%	100	100	100	100

New Data Testing After Training

Actual Class of Observation

	Normal	Abnormal	Total	P2%
Normal	5	2	7	71
Abnormal	0	1	1	100
Total	5	3	8	85
P1%	100	33	67	76

NOTE: P1: p(prediction=x, actual=x), P2: p(actual=x, prediction=x)

Table 6. Neural Networks Results of ROTOR.DB
a. for Y-Response

Raw Data (Y-Force of ROTOR.DB, Received on Feb 18,1993)
After 300 training cycles
Random Selection of Training Data Sets

Self-Testing After Training

Actual Class of Observation

	Normal	Abnormal	Total	P2%
Normal	6	0	6	100
Abnormal	0	1	1	100
Total	6	1	7	100
P1%	100	100	100	100

New Data Testing After Training

Actual Class of Observation

	Normal	Abnormal	Total	P2%
Normal	6	1	7	86
Abnormal	0	1	1	100
Total	6	2	8	93
P1%	100	50	75	84

NOTE: P1: p(prediction=x, actual=x), P2: p(actual=x, prediction=x)

Table 6. Neural Networks Results of ROTOR.DB
b. for Y-Force